TU Delft

Bachelor final project
Mathematics and Physics

Analysis of a Nonlinear Rouse Model

D.J. van Dijk

supervised by
Johan Dubbeldam
and
Marileen Dogterom

September 6, 2018

Preface

This Bachelor Final Project is largely inspired by a paper of Vandebroek-Vanderzande [3]. This paper is about how a Rouse polymer behave in a crowded environment such as a human cell. Or as the title of their paper puts it; *the dynamics of a polymer in an active and viscoelastic bath.*

This title sounds quite technical. As this thesis should be readable by my peers, i.e. final year mathematics and physics bachelor students, some background information should be provided. This will be done in the first chapter. In this chapter the reader will be introduced to concepts such as: Brownian motion, the Rouse model and Rouse modes.

In the second chapter a variation on the Rouse model will be introduced: a semiflexible chainmodel. In this model the angles between particles in the polymer play an important role. From first sight it's not clear what kind of implications this adjustment has. By performing numerical simulations I'll try to give an answer to this. I would like to advert that the code for the simulations can be found online at: `https://github.com/daanvandijk/polymers`.

In the third chapter the semiflexible chainmodel will be studied from an analytical perspective. By using an Adomian decomposition scheme a short time limit will be derived. This will give a quantitative understanding of the behavior of the semiflexible chainmodel in short time-frames.

At last I would like to take this opportunity to thank my main supervisor Johan Dubbeldam. Collaborating with you has been very pleasant. I don't know many people who react more enthusiastically and encouraging to my ideas. Even when life kicked back for me personally and I had to take a break from this project, you reacted very calmly. Know that I'm appreciative and grateful for that.

Contents

Notation

This is a summary of some of the notation used throughout the thesis. Notice that vectors have no typographic indication; they are not boldfaced or have arrows above them. When quantities such as position and force are considered, the reader should keep in mind that these are 3 dimensional. Inner products are notated with a dot. On the other hand, quantities such as angles and energy are just scalars.

- The letter t is associated with time.
- R is associated with position.
- The letter ξ is associated with stochastic forces. In the discrete models $\xi_n(t) = \xi_{x,n}\hat{x} + \xi_{y,n}\hat{y} + \xi_{z,n}\hat{z}$ denotes the stochastic force working on the n^{th} particle. In the continuous model this is notated as $\xi(n,t)$.
- The letter U is associated with potentials.
- The letter θ is associated with angles.
- The constants $k > 0$ and $a > 0$ are associated with the spring- and angle-potentials respectively.
- The constant $l > 0$ is associated with average length between particles.
- The letter N is associated with: the number of timesteps N_t or the number of particles N_p.
- Expectations of stochastic variables will be notated with angle notation, e.g. $\langle \xi \rangle$.

1 Introduction

1.1 Motivation

Before going in-depth into all the mathematics and physics, there should be some motivation. *Why* is polymer dynamics worth studying?

In essence; carbon life is all about polymers! From RNA and DNA to cellulose to carbohydrates. Carbon life indeed relies a lot on polymers.

We already know a lot about how polymers behave in a not-so-crowded environment. That is; in the statistical physics kind of way; we can successfully predict diffusion speeds outside of cells. But it's much harder to describe what happens in the inside of cells. It's quite hard to study the living contents of cells. You cannot simply cut it open and see what happens the same way you would open a cuckoo-clock and see it's internal mechanism ticking away. The scale of cells is simply too small. And furthermore breaking open a cell would disturb it's processes. So therefore there's need for models that make predictions.

1.2 Brownian motion

Historically speaking *Robert Brown* was the first person to investigate stochastic motion. In 1827 he studied small pollen of grains in water which moved in a very irregular way. It was not until 1905 before *Albert Einstein* could give a satisfactory explanation for the stochastic motion [13]. The pollen were being moved by collisions with individual water molecules. This reasoning was one of the first convincing arguments for the evidence of molecules and atoms. Einstein and others, such as *Paul Langevin*, derived that these pollen should diffuse with speed $\sigma_{\text{cm}} \propto \sqrt{t}$.

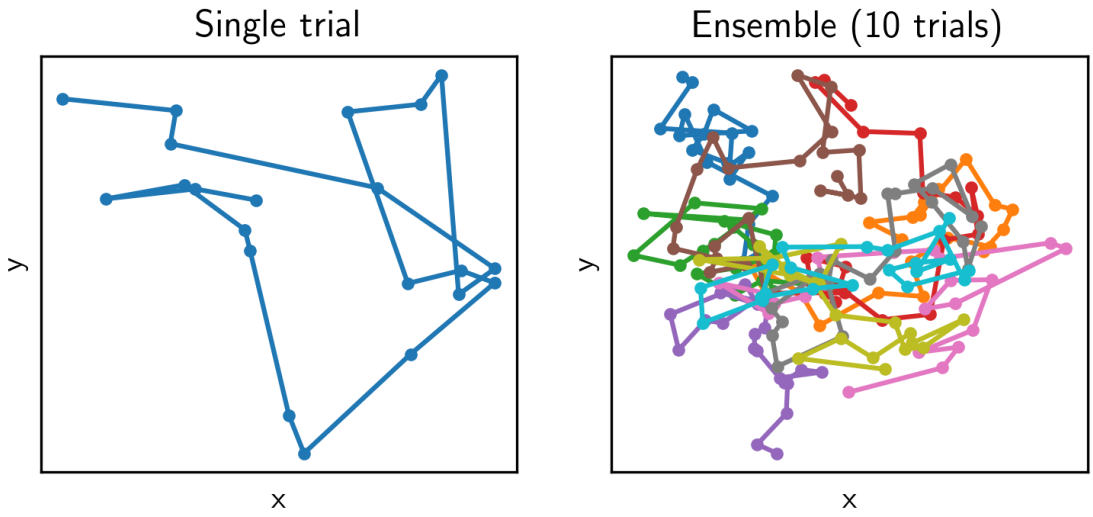

Figure 1: On the left a single trial of Brownian motion is showed in the x, y-plane for a certain time t. On the right a small ensemble of Brownian trials is showed. Notice how over time the particles in the ensemble start moving away from the origin. This spreading out is often referred to as *diffusion*.

1.3 Rouse model

The Rouse Model is one of the first models that tries to describe the dynamics of polymers. It was proposed by Prince E. Rouse in 1953. In essence it's a chain of Rouse beads connected to each other via harmonic springs. Its use is to give insight in certain statistical

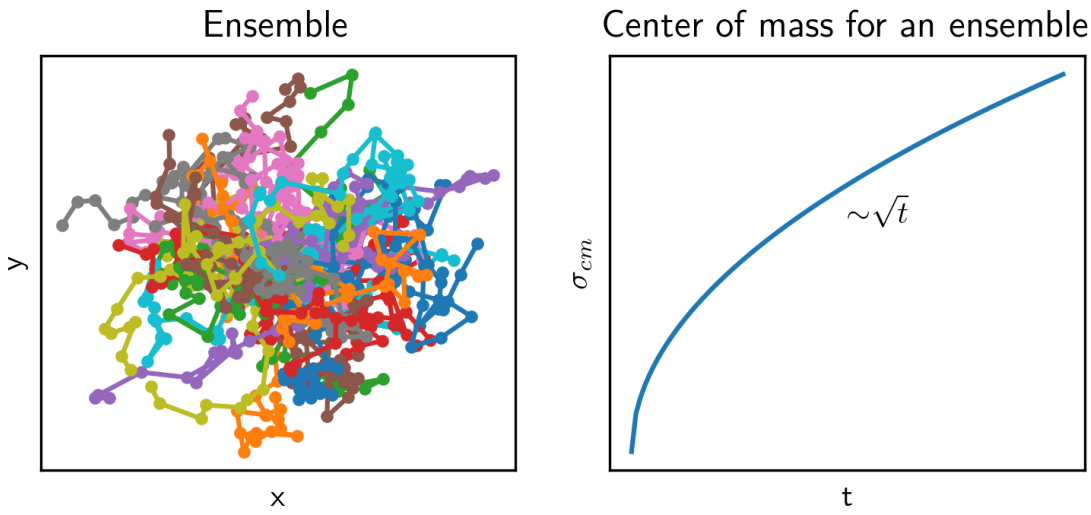

Figure 2: On the left an ensemble of Brownian motion is showed. It can be derived that the diffusion factor σ_{cm} is proportional to $\sqrt{t}$.

physics questions, such as: "*how fast do polymers diffuse?*" Although the Rouse model is relatively simple, it successfully predicts the long-time diffusion factor.

So consider N_p point mass-particles connected together via springs. The system of equations then reads:

$$\frac{\partial R_n}{\partial t} = -k(2R_n - R_{n+1} - R_{n-1}) + \xi_n(t) \tag{1}$$

where R_n is the position of the n-th particle; $n \in \{0, 1, .., N_p - 1\}$. The boundary conditions arise from the fact that this chain is open-ended;

$$\begin{cases} R_0 = R_{-1} \\ R_{N_p-1} = R_{N_p} \end{cases} \tag{2}$$

The 'particles' R_{-1} and R_{N_p} are sometimes called phantom beads, since they don't really exists. The stochastic forces are normally distributed and characterized by their first- and second-moments:

$$\begin{cases} \langle \xi_n(t) \rangle = 0 \\ \langle \xi_n(t) \cdot \xi_m(t') \rangle = \delta_{n,m}\delta(t - t') \end{cases} \tag{3}$$

where δ is the Dirac-delta function. The yielded diffusion factor of the Rouse model is, similar to a single Brownian particle:

$$\sigma_{cm} \propto \sqrt{t} \tag{4}$$

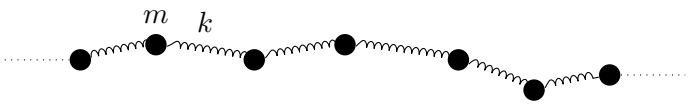

Figure 3: An illustration of the Rouse model: a series of pointmasses m connected with springs k to their two nearest neighbors.

1.4 Rouse modes

An important tool for studying the Rouse model are the so called Rouse modes. The transform is given by:

$$X[R_n] = \frac{1}{N_p} \sum_{n=0}^{N_p-1} R_n \cos\left(\frac{\pi p(n+1/2)}{N_p}\right), \quad n, p \in \{0, 1, ..., N_p - 1\} \tag{5}$$

And the inverse transform is given by:

$$X^{-1}[X_p] = \sum_{|p|<N_p} X_p \cos\left(\frac{\pi p(n+1/2)}{N_p}\right) \tag{6}$$

It's helpful to realize that the Rouse modes are in essence a Fourier series transform *such that* the boundary conditions 2 of the Rouse model are satisfied. Therefore it also inherits all the properties of Fourier series. For more details about how to derive these modes see Appendix B.

Remark 1.1 (Notation). In texts such as [2] and [3] the notation X_p for $X[R_n]$ is used.

Remark 1.2. In the Rouse mode domain, one can linearize the system of equations given by (1), that is

$$\frac{\partial X_p}{\partial t} = -k_p X_p + \xi_p \tag{7}$$

After an explicit solution for X_p is found, one can transform back to R_n. This is one of many examples where it's easier to solve a problem in the Fourier domain.

Remark 1.3. Notice that the center of mass is given by the first Rouse mode, i.e.

$$X_0 = \frac{1}{N_p} \sum_{n=0}^{N_p-1} R_n = R_{\text{cm}}$$

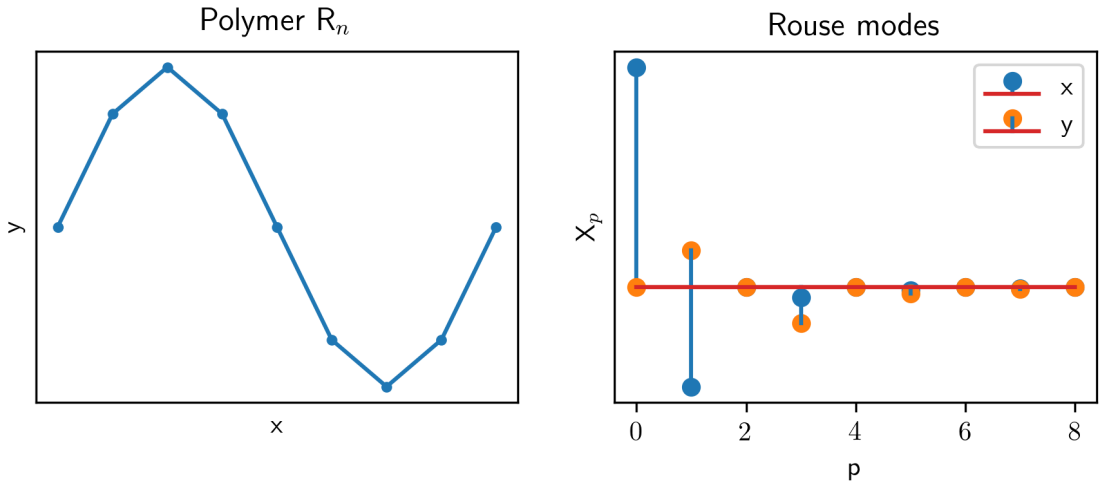

Figure 4: An example of a (non-important) 2D polymer R_n and it's Rouse modes X_p. These modes were obtained by evaluating the transform 5 for the x- and y-direction. Notice that the left and the right side contains equal amount of information. I.e. on the left side there are 9 points $R_n = (x_n, y_n)$. And on the right side there are 9 Rouse modes in the x-direction and 9 Rouse modes in the y-direction. Furthermore notice that the zeroth Rouse mode in the y-direction is 0. This is because the center of mass in the y-direction is 0.

Remark 1.4. Notice that it's in some sense easier to look at a plot in Rouse space compared to Euclidean space (see for example figures 4 and 5). Especially if it's 3 dimensional Euclidean space. Depth is something that can be easily misinterpreted. I.e. a 2D projection of 3D euclidean space loses information while on the other hand the Rouse modes do not.

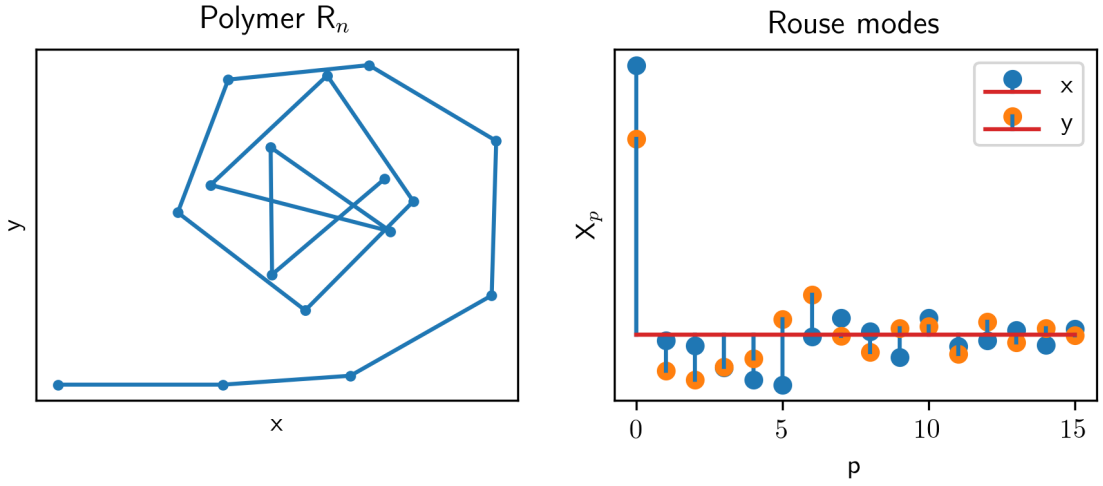

Figure 5: Another example of a (non-important) polymer R_n and it's Rouse modes X_p. Notice that this polymer contains more higher-frequency modes than the one in figure 4. This can also be seen in real space; the polymer R_n in this figure is much more entangled than the one in figure 4. Moreover the center of mass in the y-direction is not 0, unlike figure 4.

1.5 Statistical quantifiers

There should be some regard to the statistical quantifiers that are often regarded in polymer dynamics. As was showed earlier, one of the quantities people are often interested in is the center of mass of polymers since this is a measure for diffusion. For a Rouse polymer with N_p point-masses the center of mass R_{cm} is classically defined as

$$R_{\text{cm}}(t) = \frac{1}{N_p} \sum_{n=0}^{N_p-1} R_n(t) \tag{8}$$

It's first and second moment are then given by

$$\mu_{\text{cm}}(t) = \langle R_{\text{cm}}(t) \rangle = \frac{1}{N_p} \sum_{n=0}^{N_p-1} \langle R_n(t) \rangle \tag{9}$$

$$\sigma_{cm}^2(t) = \langle (R_{\text{cm}}(t) - R_{\text{cm}}(0))^2 \rangle - \langle R_{\text{cm}}(t) - R_{\text{cm}}(0) \rangle^2 \tag{10}$$

Another interesting statistical quantifier is the normed end-to-end length.

$$R_{\text{ee}} = \frac{|R_0 - R_{N_p}|}{\sum_{n=0}^{N_p-1} |R_n - R_{n+1}|} \tag{11}$$

Notice $0 \leq R_{\text{ee}} \leq 1$. When $R_{\text{ee}} = 1$, the polymer is in a stretched state, just like uncooked spaghetti. When R_{ee} is very small, then the polymer is in a very entangled state.

Remark 1.5. Notice that even though R_n is usually 3-dimensional, quantifiers such as $\sigma_{cm}(t)$ often gets plotted along only one axis (e.g. figure 7). The reason for this is that the considered equations of motion do not favor any direction of space in any sense. I.e. $\sigma_{cm}(t) \cdot \hat{x}$ will be proportional to $\sigma_{cm}(t) \cdot \hat{y}$ etc. And since we often only care about the order of t plotting the mean of the three directions $\sigma_{cm}(t)$ (or even only one direction $\sigma_{cm}(t)$, say $\sigma_{cm}(t) \cdot \hat{x}$) seems reasonable enough.

1.6 The model of Vandebroek-Vanderzande

This thesis was largely inspired by [3]. Before stating their results, first a small summary of their model. They also consider an open Rouse chain of a fixed number of particles.

The equation of motion of the n-th particle reads:

$$\int_0^t K(t-\tau)\frac{dR_n(\tau)}{dt}d\tau = -k\left(2R_n(t) - R_{n+1}(t) - R_{n-1}(t)\right) + \xi_{T,n}(t) + \xi_{A,n}(t) \tag{12}$$

with the memory kernel $K(t)$ (for the interested reader, see: [10])

$$K(t) = (2-\alpha)(1-\alpha)t^{-\alpha}, \quad 0 < \alpha < 1. \tag{13}$$

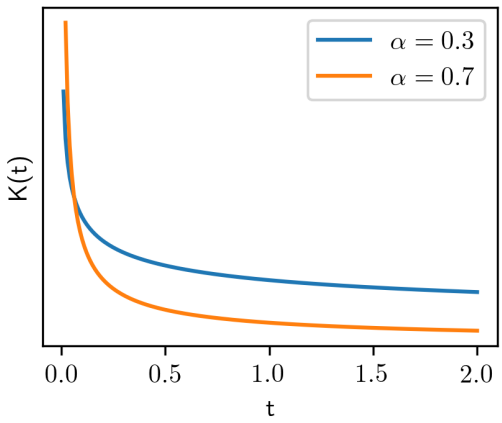

Figure 6: The kernel function $K(t)$ for several values of α. The intuition is as follows: For a high value of α the information from the past is relatively unimportant. For a low value of α the information from the past is relatively important.

Here $\xi_{T,n}(t)$ and $\xi_{T,n}(t)$ are normally-distributed stochastic variables, with expectation:

$$\langle \xi_{T,n} \rangle = \langle \xi_{A,n} \rangle = 0 \tag{14}$$

The thermal force $\xi_{T,n}(t)$ acting on the n-th monomer has its correlation coupled with the kernel $K(t)$ by the second fluctuation-dissipation theorem

$$\left\langle \xi_{T,n}(t) \cdot \xi_{T,m}(t') \right\rangle = 3k_B T K(|t-t'|)\delta_{n,m}. \tag{15}$$

The active force $\xi_{A,n}(t)$ acting on the n-th monomer has an assumed correlation of

$$\left\langle \xi_{A,n}(t) \cdot \xi_{A,m}(t') \right\rangle = 3C\exp(-|t-t'|/\tau_A)\delta_{n,m}. \tag{16}$$

Here C characterizes the strength of the active noise, and τ_A gives information about the timescale of the active forces.
The kernel function for several values of α is shown in figure 6. Note that if $\alpha \to 1$, then $K(t) \to \delta(t)$. This results in viscous behavior. For viscous behavior the equations of motion read:

$$\frac{dR_n}{dt} = -k(2R_n(t) - R_{n+1}(t) - R_{n-1}(t)) + \xi_{T,n}(t) + \xi_{A,n}(t) \tag{17}$$

Remark 1.6. In general the kernel $K(t)$ doesn't work well in a numerical time-integration scheme. I.e. the exponential behavior of the kernel throws a spanner in the works and should be dealt with care. For that reason I only consider the case $K(t) = \delta(t)$.

Remark 1.7. In conclusion, the essential difference between Rouse model and Vanderzande-Vandebroek is: 1) the introduction of active forces, and 2) the memory kernel $K(t)$.

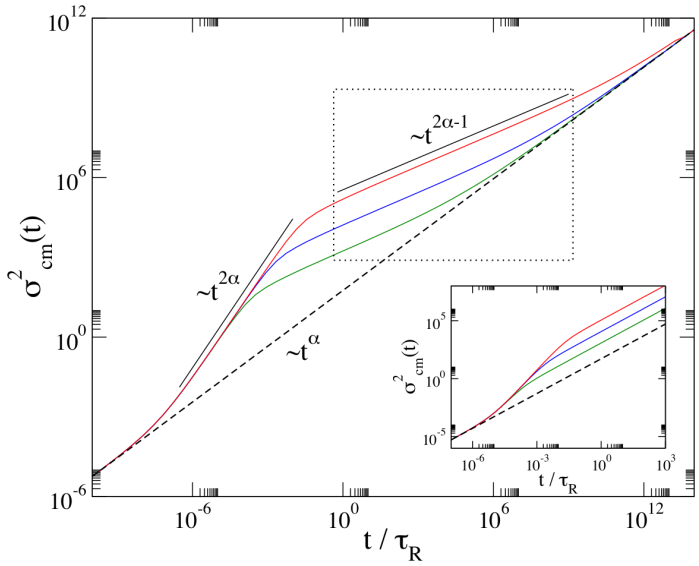

Figure 7: Log-log plot of the centre of mass as a function of time for a Rouse chain in a viscoelastic medium ($\alpha = 0.7$) in the presence of active forces. Compared to that without active forces (dashed line). The inset shows the same for the viscous case, $\alpha = 1$. (Source: [3])

Now that the model is introduced their results can be discussed. The active forces on small time-scales, w.r.t. the rouse time τ_R, induce a faster diffusion rate. In comparison to a model without active forces, this rate is squared. This can be seen in figure 7. For large time-scales this diffusion rate asymptotically goes back to the regular rouse model. The term for this high diffusion rate, coined by the authors, is *superdiffusion*. The authors compared their model to experimental studies. Chromosomal loci in the bacteria E. Loci move very rapidly. It isn't yet clear if this is due to active processes or can be explained by other reasons such as stress relaxation.

2 Semiflexible chain model

2.1 Motivation

In all the previous models described there was never a restriction set on the angle between successive particles. Surely these angles can not be arbitrarily. One would expect that if a polymer has a breaking point; if the angle between particles becomes too large the string would just break. There are numerous ways of taking such behavior into account. In the model proposed here we introduce an angle potential.

This introduces some sort of 'penalty' on the angle between particles; the angle induces a force that pushes particles back to a low energy state. Qualitatively speaking: when the angle between particles becomes larges also the induced force becomes larger.

It is important to understand that this penalty still allows for arbitrary states. There is nothing that says that certain states are not allowed. And there is also still no breaking point of any kind. The only thing this new angle potential does is inducing a force that minimizes the angle between particles.

2.2 Energy relation

Let's say we have N particles with positions $\{R_n\}_{n=1}^N$ In this model the particles behave according to the following energy equation:

$$U = \frac{k}{2}\sum_{n=1}^{N-1} |R_n - R_{n+1} - l_n|^2 + \frac{a}{2}\sum_{n=2}^{N-1}(1-\cos\theta_n)^2 \tag{18}$$

Here θ_n is the angle between particles $(n-1), n, (n+1)$, see figure 8. Furthermore, the values $l_n > 0$ are parameters of the model[1]. They denote the steady-state length between particles n and $n+1$. Usually $l_n = l$, the same for every particle. The term $\cos\theta_n$ can be expressed in the positions of the particles $\{R_n\}_{n=1}^N$. Define

$$u_n := R_n - R_{n-1} \tag{19}$$

We consider a 3-dimensional universe. The geometric interpretation of the inner product states that:

$$\cos\theta_n = \frac{u_n \cdot u_{n+1}}{|u_n| \cdot |u_{n+1}|} \tag{20}$$

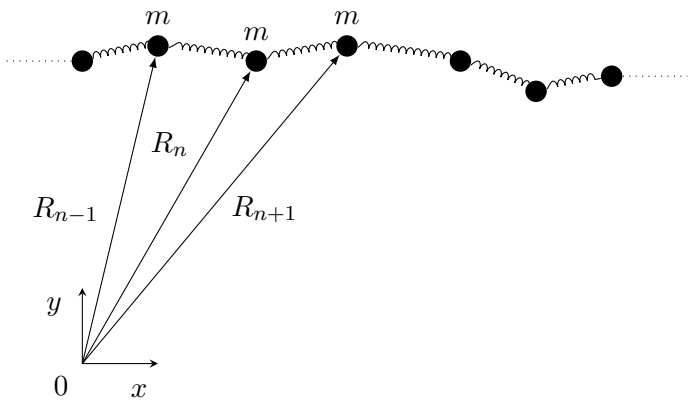

Figure 8: Here you can see how θ_n is defined from u_n.

Substituting this back in (18) yields:

$$U = \frac{k}{2}\sum_{n=1}^{N-1} |R_n - R_{n+1} + l_n|^2 + \frac{a}{2}\sum_{n=2}^{N-1}\left(1 - \frac{u_n \cdot u_{n+1}}{|u_n| \cdot |u_{n+1}|}\right)^2 \tag{21}$$

[1]Without l_n, the numerical simulations would be unstable.

Let's define R_n in terms of it's components along the x, y, z-axes:

$$R_n(t) := x_n(t)\hat{x} + y_n(t)\hat{y} + z_n(t)\hat{z}.$$

The total energy U together with the random forces $\{\xi_n(t)\}_{n=1}^N$ induce a force working on every particle R_n with $n \in \{1, ..., N\}$:

$$F_n = -\nabla_n U + \xi_n(t), \text{ where } \nabla_n U := \frac{\partial U}{\partial x_n}\hat{x} + \frac{\partial U}{\partial y_n}\hat{y} + \frac{\partial U}{\partial z_n}\hat{z}.$$

The stochastic force working on the n^{th} particle is given by:

$$\xi_n(t) = \xi_{T,n}(t) + \xi_{A,n}(t)H(t). \tag{22}$$

Here $H(t)$ is the Heaviside step function. Just like in the model of Vandebroek-Vanderzande $\xi_{T,n}(t)$ represents the thermal force and $\xi_{A,n}(t)$ represents the active force. They are given by:

$$\langle \xi_{T,n}(t) \cdot \xi_{T,m}(t') \rangle = 3k_B T \delta(|t - t'|)\delta_{n,m} \tag{23}$$

$$\langle \xi_{A,n}(t) \cdot \xi_{A,m}(t') \rangle = 3C \exp(-|t - t'|/\tau_A)\delta_{n,m} \tag{24}$$

Remark 2.1. Note that the resulting equation looks very much the same as the viscous limit of Vandebroek-Vanderzande (17). I've chosen to not consider the exponential memory kernel $K(t)$, because this makes numerical simulations much harder.

2.3 Force relation

In appendix A the explicit terms for the force relation were:

$$\nabla_n \left(\frac{k}{2} \sum_{i=1}^{N-1} |R_i - R_{i+1} - l_i|^2 \right) = k(R_n - R_{n-1}) \left(1 - \frac{l}{|R_{n-1} - R_n|} \right) + k(R_n - R_{n+1}) \left(1 - \frac{l}{|R_{n+1} - R_n|} \right) \tag{25}$$

And

$$\begin{aligned} \frac{-F_{\text{angle},n}}{2a} &= \sin(\theta_{n-1}/2) \cdot \left(R_{n-2} - R_{n-1} - \cos(\theta_{n-1}) \frac{R_{n-1} - R_n}{|R_n - R_{n-1}|^2} \right) \\ &+ \sin(\theta_n/2) \cdot \left(2R_n - R_{n-1} - R_{n+1} - \left(\frac{R_{n+1} - R_n}{|R_n - R_{n+1}|^2} + \frac{R_{n-1} - R_n}{|R_n - R_{n-1}|^2} \right) \cos(\theta_n) \right) \\ &+ \sin(\theta_{n+1}/2) \cdot \left(R_{n+2} - R_{n+1} - \cos(\theta_{n+1}) \frac{R_{n+1} - R_n}{|R_n - R_{n+1}|^2} \right) \end{aligned} \tag{26}$$

Proposition 2.1. *The equilibrium solution described by*

$$\frac{\partial R_n}{\partial t} = -k(2R_n - R_{n+1} - R_{n-1}) - F_{n,angle}$$

is stable.

Remark 2.2. Chapter 4.3 from [6] gives conditions for the stability of equilibrium solutions of non-linear systems. I.e. consider a nonlinear-system $\dot{x} = Ax + g(x)$. Suppose $g(x)/\max\{|x_1|, ..., |x_n|\}$ is a continuous function and vanishes for $x = 0$. Then the equilibrium solution $x(t) = 0$ is asymptotically stable if all the eigenvalues of A have negative real part.

Proof. Notice that the system can be transformed to Rouse coordinates:

$$\frac{\partial X_p}{\partial t} = -k_p X_p - F_{p,\text{angle}}$$

where $k_p = 4k \sin^2\left(\frac{\pi p}{2N}\right)$. In particular, for the zeroth Rouse mode:

$$\frac{\partial X_0}{\partial t} = \frac{\partial R_{\text{cm}}}{\partial t} = -F_{0,\text{angle}}$$

First considering the Rouse modes excluding the zeroth mode:

$$\begin{pmatrix} \partial X_1/\partial t \\ \vdots \\ \partial X_{N-1}/\partial t \end{pmatrix} = \begin{pmatrix} -k_1 & & 0 \\ & \ddots & \\ 0 & & -k_{N-1} \end{pmatrix} \begin{pmatrix} X_1 \\ \vdots \\ X_{N-1} \end{pmatrix} + \text{“non-linear terms”}$$

Clearly, all of the eigenvalues of A are negative. Furthermore, by definition, the non-linear terms will vanish for the equivalence class of when the angles between particles are 0. Therefore, the system excluding the zeroth Rouse mode is stable. The zeroth Rouse mode must also be stable, since for small angles, the non-equilibrium term will vanish. □

2.4 Simulations

2.4.1 Time integration-scheme

In order to evaluate this problem numerically, it needs to be discretized in time. If a Euler-forward time integration scheme was going to be used, then the equations would look as follows:

$$\begin{aligned} R_n(t+\Delta t) - R_n(t) = &-k\Delta t(2R_n(t) - R_{n+1}(t) - R_{n-1}(t)) \\ &- a\Delta t \cdot (1 - \cos\theta_{n+1}) \cdot F_n^{+1} \\ &- a\Delta t \cdot (1 - \cos\theta_n) \cdot F_n^{0} \\ &- a\Delta t \cdot (1 - \cos\theta_{n-1}) \cdot F_n^{-1} \\ &+ \sqrt{\Delta t}(\xi_{T,n}(t) + \xi_{A,n}(t)) \end{aligned}$$

Note the square root before the stochastic function. This is due to the fact that this is a Brownian motion process. By practically experimenting the Euler-forward scheme didn't converge fast enough. Instead the Runge-Kutta4 method, as described in [7] was used:

$$\begin{aligned} k_{1,n} &= F\left(\{R_n(t)\}_{n=1}^{N_p}\right) \\ k_{2,n} &= F\left(\{R_n(t)\}_{n=1}^{N_p} + \frac{k_{1,n}}{2}\right) \\ k_{3,n} &= F\left(\{R_n(t)\}_{n=1}^{N_p} + \frac{k_{2,n}}{2}\right) \\ k_{4,n} &= F\left(\{R_n(t)\}_{n=1}^{N_p} + k_{3,n}\right) \end{aligned}$$

And finally

$$R_n(t+\Delta t) - R_n(t) = \Delta t \frac{k_{1,n} + 2k_{2,n} + 2k_{3,n} + k_{4,n}}{6} + \sqrt{\Delta t}\xi_n(t)$$

Initial condition

What is a good initial condition to choose? One should spent some time on this question. Because of the potential in which the polymers live, a polymer has a certain amount of

entropy. Choosing a high entropy state as an initial condition would skew the results. Based on the parameters k_BT, k, a, C and l the following initial condition was defined:

$$|R_n - R_{n+1}| \sim \mathcal{N}(\mu_l, \sigma_l)$$
$$\theta_n \sim \mathcal{N}(\mu_\theta, \sigma_\theta)$$

For a reference of the precise numerical values, see table 1.

Name	N_p	N_t	dt	a	k	C	k_BT	l	μ_l	σ_l	μ_θ	σ_θ	Trials
Rouse model	64	1e+05	1e-08	0	1e+05	0	1e-07	1e-07	1e-07	2e-08	0	0	100
Rouse model	64	1e+05	1e-05	0	1e+05	0	1e-07	1e-07	1e-07	2e-08	0	0	100
zande-broek	64	1e+05	1e-07	0	1e+05	1e-06	1e-07	1e-07	1e-07	2e-08	0	0	100
Semiflexible	64	1e+05	1e-07	10	1e-06	1e-06	1e-07	1e-07	1e-07	2e-08	0	0	100
Semiflexible	64	1e+05	1e-08	10	1e-06	0	1e-07	1e-07	1e-07	2e-08	0	0	100

Table 1: Experiment parameters

2.5 Stability of the simulations

For the simulations it's important to know how large the timestep can be. For a linear model, it's relatively straightforward to determine this based on the differential equation and time-integration scheme. For the problem under consideration here, this was not so easy.

First of all, the system is not linear, i.e. $\frac{dR_n}{dt}$ can not be written as $\frac{dR_n}{dt} = A \cdot [R_1 ... R_{N_p}]^T + g(t)$, where A would be a matrix. I.e. equation 26 can not be written that way. So methods such as Richardson error estimation as described in [7] will not work.

Secondly, the system has a stochastic part. So directly comparing polymer trials with each other makes not really sense. Since there is not one unique solution where every initial condition will converge towards.

What does make sense however was comparing the statistical quantifiers with each other. One can check if they are reasonably smooth and follow predictions of the theory. If these are not smooth enough one can simply do the experiments again with a smaller timestep.

2.5.1 Difficulties of the simulations

Notice these simulations are not a light computing task. Just to get an idea of the scale and difficulties of the simulations:

- Let's say an ensemble of 100 polymers is considered.
- Every polymer is built up of 64 particles and is 3 dimensional.
- The number of time steps is $1e5$. Notice that for the Runge-Kuta4 scheme, in some sense, this results in 4 times as many actual steps.

If everything is a double datatype, then the amount of data that passes through the system is in the order of

$$100 \cdot (64 \cdot 3) \cdot (4 \cdot 1e5) \cdot (8 \text{ bytes per double}) = 46 \text{ Gigabyte}$$

Furthermore also the stochastic forces also need to be generated, i.e.

- For the thermal forces $1e5$ points must be generated.
- The active forces need to be exponentially auto-correlated with itself. So for every timestep a multivariate conditional normal distribution must be calculated.

I won't go into further details. The interested reader can lookup the source code online.

2.5.2 Speeding up Matlab code

Initially I wrote all of the simulations in Matlab. I quickly noticed that these took too long to finish. This can be explained by the fact that Matlab isn't very well optimized. Things such as for-loops or function calls take relatively long when compared to a language such as C.

It was possible to automatically, after some tweaking, convert all of the Matlab code to C++, with the *Matlab Coder applet*. This applet generates C++ code and compiles it into a MEX function, which in turn can be called like a regular function from Matlab itself. By doing this the initial Matlab code was sped-up by a factor of approximately 300 times.

However, the compiling of the MEX took quite a long time; approximately 30 seconds. This made quickly editing a testing code quite frustrating. Furthermore, it wasn't possible to enable multithreading. Simulating polymers is something that can easily be done in parallel. This can improve the simulation time by a factor equal to the number of threads available on the system.

Therefore, in the end, I wrote a native C++ application for all of the simulations. This can be found online. There's Matlab and Python integration. Meaning that the user can import the experiments performed by the C++ code directly into the Matlab and Python environment. So data-analysis and plots can be performed by Matlab and Python.

2.6 Simulations results

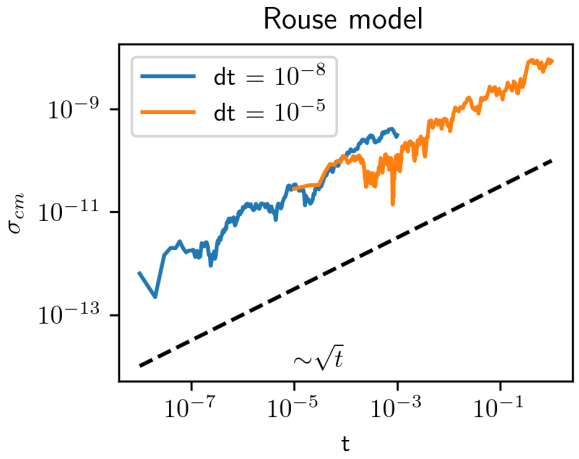

Figure 9: Comparison of the diffusion between two Rouse model ensembles with different time-steps, showing the stability of the simulations.

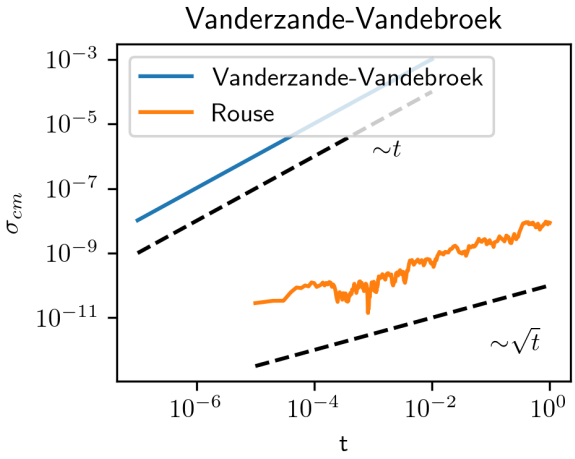

Figure 10: The diffusion for the Vanderzande-Vandebroek model compared with the Rouse model. Notice the drop-off of Vanderzande-Vandebroek at large times, just like in figure 7

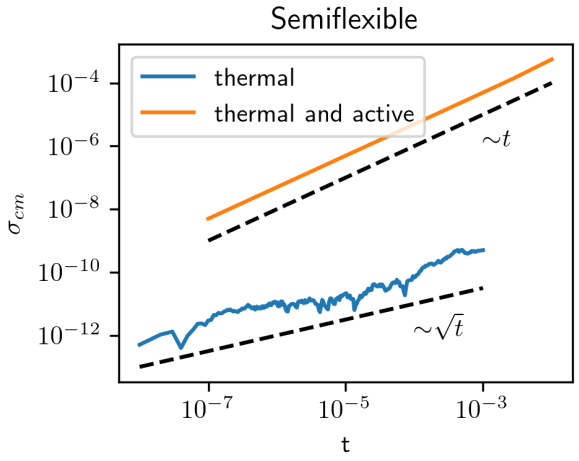

Figure 11: The diffusion for the semiflexible chainmodel, for an ensemble with- and without active forces.

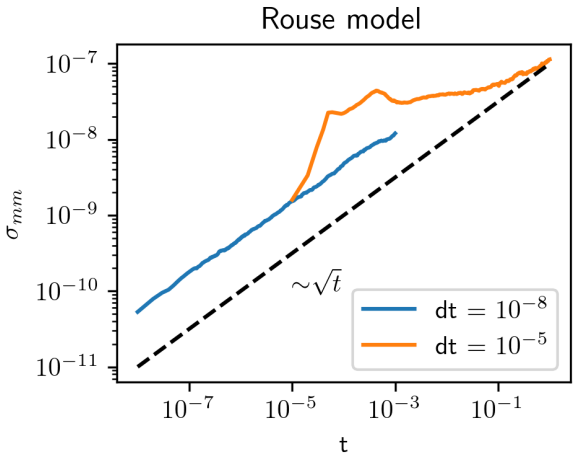

Figure 12: The diffusion of the middle monomer for the Rouse model.

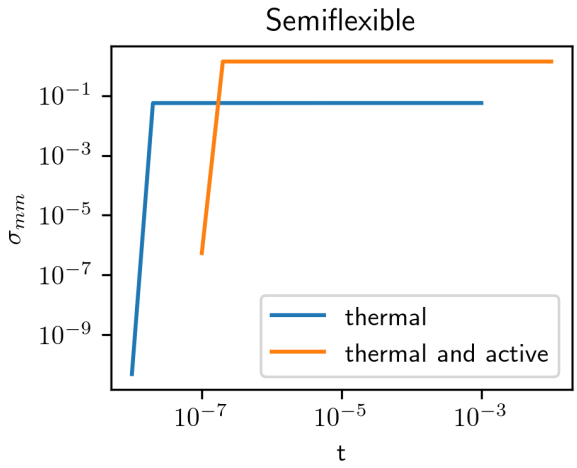

Figure 13: The diffusion of the middle monomer for the semiflexible model. Notice the nonlinear behavior for small time steps.

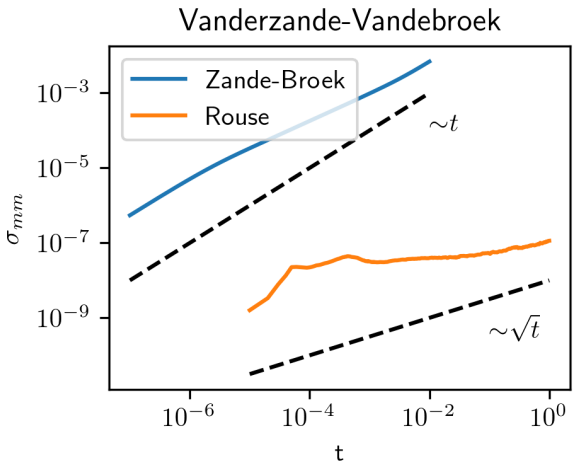

Figure 14: The diffusion of the middle monomer for the Vanderzande-Vandebroek model.

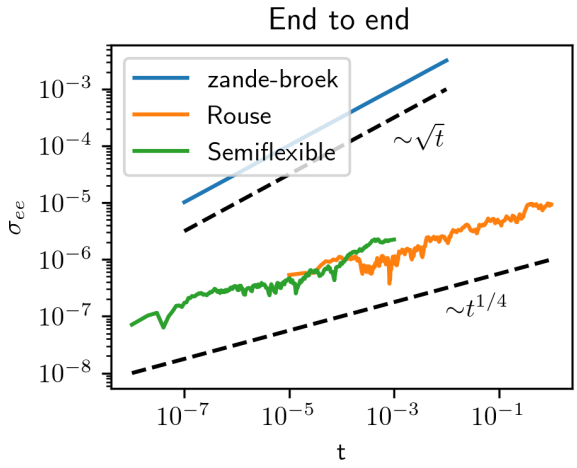

Figure 15: A comparison between the variance of the end-to-end R_{ee} distance of the three models. The semiflexible model plotted here is non-active.

3 Adomian decomposition

3.1 Motivation

The goal of this chapter is to study the semiflexible chainmodel from a analytical perspective. Quite naturally the first thing I tried was directly applying perturbation theory. As it turns out, the yielded system of equations was, as far to my knowledge, too hard to work with. For the interested reader, the details of this trial are in remark 3.1. The next thing to attempt was making the model continuous. As it turns out, some of the difficulties disappear then. I.e. dealing with $\partial^2 R/\partial n^2$ is easier than with $2R_n - R_{n+1} - R_{n-1}$.

Remark 3.1 (First failed attempt). Recall $u_n = R_n - R_{n-1}$. In the spirit of perturbation theory consider $u_n = l_n + \varepsilon_n$. Assume $|u_n| \approx l$, the average length between neighbors. Of course, one is not concerned about the linear part of the model. So, let's try to approximate the angle force. For F_n^0 this yields:

$$\begin{aligned} F_n^0(u_n, u_{n+1}) &= \frac{u_n - u_{n+1}}{|u_n| \cdot |u_{n+1}|} + \left(\frac{u_n}{|u_n|^2} - \frac{u_{n+1}}{|u_{n+1}|^2} \right) \frac{u_n \cdot u_{n+1}}{|u_n| \cdot |u_{n+1}|} \\ &\approx \frac{u_n - u_{n+1}}{l^2} + \left(\frac{u_n}{l^2} - \frac{u_{n+1}}{l^2} \right) \frac{u_n \cdot u_{n+1}}{l^2} \\ &= \frac{u_n - u_{n+1}}{l^2} \left(2 + \frac{u_n \cdot u_{n+1}}{l^2} \right) \end{aligned}$$

And F_n^{-1}

$$\begin{aligned} F_n^{-1}(u_{n-1}, u_n) &= \frac{u_{n-1} \cdot u_n}{|u_{n-1}| \cdot |u_n|} \frac{u_n}{|u_n|^2} - \frac{u_{n-1}}{|u_{n-1}| \cdot |u_n|} \\ &\approx \frac{u_{n-1} \cdot u_n}{l^2} \frac{u_n}{l^2} - \frac{u_{n-1}}{l^2} \end{aligned}$$

Now consider

$$\frac{\partial u_n}{\partial t} = -k(2u_n - u_{n+1} - u_{n-1}) - F_{n,angle}(u_{n-1}, u_n, u_{n+1}) + \xi_n$$

Where $F_{n,angle}(u_{n-1}, u_n, u_{n+1})$ is a linear combination of $F_n^{-1}, F_n^0, F_n^{+1}$. It was not obvious to me how one progresses from here.

3.2 Introduction

As said in the motivation, one way to progress further, is to make the discrete model continuous. The system of stochastic ordinary differential equations will then become stochastic partial differential equation. In table 2 a comparison between these two models is made.

Remark 3.2. From a strictly theoretical perspective it's not clear whatsoever that proving anything in the continuous model will also prove the same thing in the discrete model, or the other way around. But still one can reasonably expect the two models behave similarly. The argument for this is if the number of particles goes to infinity, then all of the summations over n will converge to a Riemann integral:

$$\sum_{n=0}^{\infty} ... \longrightarrow \int_{n=0}^{N_p} ...dn$$

with N_p some constant, usually taken 1.

The continuous analogue of the semiflexible chainmodel I propose is:

$$\frac{\partial R}{\partial t} = k \frac{\partial^2 R}{\partial n^2} + a \left(\frac{\partial^2 R}{\partial n^2} \right)^2 + \xi(n, t) \tag{27}$$

	Continuous	Discrete
Position notation	$R(n,t)$	$R_n(t)$
Time derivative	$\partial R/\partial t$	dR_n/dt
First-order derivative	$\partial R/\partial n$	$R_{n+1} - R_n$
Second-order derivative	$\partial^2 R/\partial n^2$	$R_{n+1} + R_{n-1} - 2R_n$
Center of mass	$\int_0^{N_p} R(n,t)dn$	$\sum_{n=0}^{N_p-1} R_n/N_p$
Rouse transform	$X[R] = \int_0^{N_p} R\cos(\pi pn/N_p)dn$	$X[R_n] = \sum_{n=0}^{N_p-1} R_n \cos(\pi p(n+1/2)/N_p)$

Table 2: Comparison of the continuous and discrete model.

with boundary conditions

$$\left.\frac{\partial R}{\partial n}\right|_{n=0} = \left.\frac{\partial R}{\partial n}\right|_{n=1} = 0 \tag{28}$$

Notice that some liberty was taken in the choice of the angle potential/force, see figure 16.

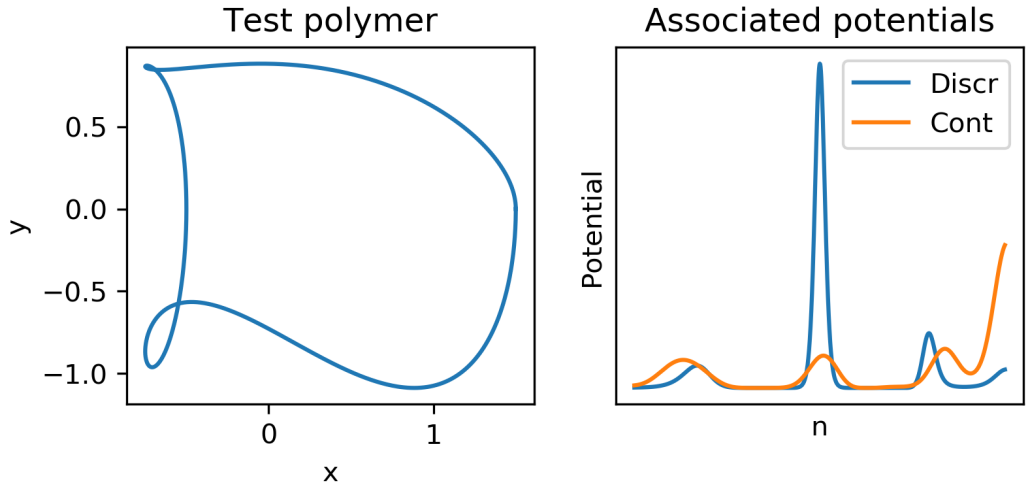

Figure 16: A comparison between the discrete potential (18) and the continuous potential (27) for some simple - and unimportant - configuration $R(n, t = 0)$. The potentials were re-scaled in order to be compared together. Notice that the peaks of both potentials are approximately at the same place, although they're surely not identical. But for a qualitative analysis, it's hoped that this is good enough. I.e. one could expect the two systems to behave similarly.

Now, as the title of this chapter suggests, this p.d.e. was further examined with the Adomian decomposition scheme, as a reference I used [11] and [12]. Without further ado:

Proposition 3.1 (Adomian decomposition scheme)**.** *Let $L(y) = N(y)$ be a non-linear differential equation with initial condition $y(0)$. Let $\{A_n\}_{n\in\mathbb{N}}$ and $\{y_n\}_{n\in\mathbb{N}}$ be two sequences defined as follows:*

$$y_0 = y(0) \tag{29}$$

$$A_n = \frac{\partial^n}{\partial\lambda^n} \frac{N(\sum_{k=0}^{n} y_k\lambda^k)}{n!}\bigg|_{\lambda=0} \tag{30}$$

$$y_{n+1} = L^{-1}(A_n) \tag{31}$$

For reasonable operators N and L one may expect that $\sum_{n=1}^{\infty} y_n = y$.

Remark 3.3. Adomian decomposition can be seen as a generalization of the Picard-Lindelöf theorem, which gives conditions for the existence and uniqueness of solutions to first-order differential equations with given initial conditions. I.e. let $L = \frac{d}{dt}$ and $N(y) = f(t, y)$. Where f is Lipschitz continuous in y and continuous in t. Then the Adomian decomposition scheme indeed becomes the same as Picard iteration. See example 3.1.

Remark 3.4. The reason that makes this scheme attractive is that the operator N is directly applied. It's often quite hard to find an inverse for N, as opposed to finding an inverse for L.

Another reason this scheme is interesting, is that it's relative easy to implement in software packages that support symbolic math. Notice that this is fundamentally different than performing numerical integration. The symbolic math method returns a series expansion and the numerical integration returns a list numerical values that approximate the solution.

Remark 3.5. Proposition 3.1 is quite vague with respect to what *reasonable* operators N and L are. Convergence can be proved for specific N and L. A standard way of doing this is proving that there is some contraction and then invoking the Banach fixed-point theorem. Just like in a standard proof of the Picard-Lindelöf theorem.

Example 3.1. Consider $L(y) = N(y)$ where $L(y) = \frac{dy}{dt}$, $N(y) = y^2$. The initial condition $y(0) = 1$. Notice that $L^{-1}(\cdot) = \int_0^t (\cdot) d\tau$.

$$
\begin{aligned}
A_0 &= N(y_0) = 1 \\
y_1 &= L^{-1}(A_0) = t \\
A_1 = \frac{\partial}{\partial \lambda} N(y_0 + \lambda y_1)\Big|_{\lambda=0} &= \frac{\partial}{\partial \lambda}(1 + 2\lambda t + \lambda^2 t^2)\Big|_{\lambda=0} = 2t \\
y_2 &= L^{-1}(A_1) = t^2 \\
A_2 = \frac{1}{2}\frac{\partial^2}{\partial \lambda^2} N(y_0 + \lambda y_1 + \lambda^2 y_2)\Big|_{\lambda=0} &= \frac{1}{2}\frac{\partial^2}{\partial \lambda^2}(\lambda^2(3t^2) + ...)\Big|_{\lambda=0} = 3t^2 \\
y_3 &= L^{-1}(A_2) = t^3 \\
A_3 = \frac{1}{6}\frac{\partial^3}{\partial \lambda^3} N(y_0 + \lambda y_1 + \lambda^2 y_2 + \lambda^3 y_3)\Big|_{\lambda=0} &= 4t^3 \\
y^4 &= L^{-1}(A_3) = t^4
\end{aligned}
$$

Listing 1: Maple implementation

```
Linv := y -> int(subs(t=s, y), s = 0 .. t);
N := y -> y^2;
y(0) := 1;
for n from 0 to 10 do
A(n) := eval(diff(N(sum(y(k)*lambda^k, k = 0 .. n))/factorial(n), [
    lambda$n]), lambda = 0);
y(n+1) := Linv(A(n));
end do;
```

3.3 Finding inverse of linear operators using Fourier transform

Definition 3.1. The Fourier transform $\mathcal{F}[\cdot]$ of a function f in Schwartz space $S(\mathbb{R}^n)$ is defined by

$$\mathcal{F}[f] \equiv \hat{f}(\xi) := \int_{\mathbb{R}^n} e^{-ix\cdot\xi} f(x) dx, \quad \xi \in \mathbb{R}^n \tag{32}$$

The inverse Fourier transformation $\mathcal{F}^{-1}[\cdot]$ is given by

$$\mathcal{F}^{-1}[\hat{f}] := (2\pi)^{-n} \int_{\mathbb{R}^n} e^{ix\cdot\xi} \hat{f}(\xi) d\xi, \quad x \in \mathbb{R}^n \tag{33}$$

Example 3.2. Consider the following linear differential operator

$$L = \frac{d}{dt} + k \tag{34}$$

Using the Fourier transform:

$$\widehat{Ly}(s) = (is + k)\hat{y}$$

Notice that $\widehat{L^{-1}} = 1/(is + k)$, since $\widehat{L^{-1}}\widehat{L} = \widehat{L}\widehat{L^{-1}} = 1$. Furthermore

$$\mathcal{F}^{-1}[L^{-1}] = \mathcal{F}^{-1}\left[1/(is + k)\right] = e^{-kt}u(t)$$

Now the relation $Ly = \gamma$ and $L^{-1} * \gamma = y$ holds. The latter can be explicitly written as:

$$\begin{aligned} L^{-1} * y &= \int_{-\infty}^{\infty} e^{-k(t-\tau)}u(t-\tau)y(\tau)d\tau \\ &= \int_{-\infty}^{t} e^{-k(t-\tau)}y(\tau)d\tau \\ &= e^{-kt}\int_{-\infty}^{t} e^{k\tau}y(\tau)d\tau \end{aligned}$$

For this example it's relatively easy to directly check that $L(L^{-1} * y) = L^{-1} * (Ly) = y$. Using the fundamental theorem of calculus:

$$\begin{aligned} L(L^{-1} * \gamma) &= \left(\frac{d}{dt} + k\right) e^{-kt}\int_{-\infty}^{t} e^{k\tau}\gamma(\tau)d\tau \\ &= e^{-kt}\frac{d}{dt}\int_{-\infty}^{t} e^{k\tau}\gamma(\tau)d\tau \\ &= \gamma(t) \end{aligned}$$

And the converse

$$\begin{aligned} L^{-1}(Ly) &= e^{-kt}\int_{-\infty}^{t} e^{k\tau}\left(\frac{dy}{d\tau} + ky(\tau)\right)d\tau \\ &= e^{-kt}\int_{-\infty}^{t} e^{k\tau}\frac{dy}{d\tau}d\tau + ke^{-kt}\int_{-\infty}^{t} e^{k\tau}y(\tau)d\tau \\ &= e^{-kt}\left[e^{k\tau}y(\tau)\right]_{-\infty}^{t} - ke^{-kt}\int_{-\infty}^{t} e^{k\tau}y(\tau)d\tau + ke^{-kt}\int_{-\infty}^{t} y(\tau)d\tau \\ &= y(t) \end{aligned}$$

So, indeed L^{-1} is found. Notice that normally checking $L(L^{-1} * y) = L^{-1} * (Ly) = y$ directly is not so easy. But this is also not necessary, since this is guaranteed by Fourier Analysis.

Remark 3.6. This method gives convergence in L^p sense, which is in turn implies convergence in $\langle\cdot\rangle$ sense.

Now reconsider the linear operator used in the continuous semiflexible chainmodel:

$$L = \frac{\partial}{\partial t} - k\frac{\partial^2}{\partial n^2}$$

Taking the two dimensional Fourier transform

$$\widehat{Lu} = (i\tau + k(i\eta)^2)\hat{u} = (i\tau - k\eta^2)\hat{u} \tag{35}$$

The goal now is to find L^{-1} by taking the inverse Fourier transform.

Proposition 3.2. *(Gaussian Fourier transform)*

$$\mathcal{F}[e^{-\alpha x^2}] = \sqrt{\pi/\alpha}e^{-\xi^2/4\alpha}, \quad \alpha > 0 \tag{36}$$

Proof. First consider $f(x) = e^{-x^2}$. Notice that

$$\begin{aligned}\frac{d}{d\xi}\hat{f}(\xi) &= \frac{d}{d\xi}\int_{\mathbb{R}} e^{-x^2}e^{-ix\xi}dx \\ &= \int_{\mathbb{R}} e^{-x^2}(-ix)e^{-ix\xi}dx \\ &= \frac{i}{2}\int_{\mathbb{R}}\left(\frac{d}{dx}e^{-x^2}\right)e^{-ix\xi}dx\end{aligned}$$

Now using integration by parts: $\int fG = FG| - \int Fg$;

$$\frac{d}{d\xi}\hat{f}(\xi) = -\frac{i}{2}\int_{\mathbb{R}} e^{-x^2}(-i\xi)e^{-ix\xi}dx = \frac{-\xi}{2}\hat{f}(\xi)$$

The solutions of the above ordinary differential equation is given by:

$$\hat{f}(\xi) = C\exp(-\xi^2/4)$$

The integration constant C can be found by: $C = \hat{f}(0) = \int_{\mathbb{R}} f(x)dx = \sqrt{\pi}$. Now using the scaling property $\mathcal{F}[f(\alpha x)] = \hat{f}(\xi/\alpha)/\alpha$, we can find $\mathcal{F}[e^{-\alpha x^2}] = \sqrt{\pi/\alpha}e^{-\xi^2/4\alpha}$. □

Now using the previous proposition gives:

$$\begin{aligned}\mathcal{F}^{-1}\left[\frac{1}{i\tau - k\eta^2}\right] &= \mathcal{F}^{-1}\left[e^{-k\eta^2 t}u(t)\right] \quad \text{(first taking the fourier inverse w.r.t. } \eta) \\ &= \frac{e^{-n^2/4kt}}{2\sqrt{\pi kt}}u(t)\end{aligned}$$

Here $u(t)$ denotes the Heaviside function. Now, there is an expression for the L^{-1} operator. It can be applied with a convolution, i.e.

$$L^{-1} * R(n,t) = \int_0^{N_p} d\eta \int_0^t d\tau \frac{e^{-(n-\eta)^2/4k(t-\tau)}}{2\sqrt{\pi k(t-\tau)}}R(\eta,\tau)$$

3.4 Applied to our model

Proposition 3.3. *Consider the continuous semiflexible chainmodel with operators*

$$\begin{aligned}L &= \frac{\partial}{\partial t} - k\frac{\partial^2}{\partial n^2} \\ N &= \left(\frac{\partial^2}{\partial n^2}\right)^2\end{aligned}$$

Let $\phi^0(n, t = 0)$ be an initial condition. Let $\{A_m(n,t)\}_{m\geq 0}$ and $\{\phi^m\}_{m\geq 0}$ be two sequences defined as

$$A_m(n,t) = \frac{\partial}{\partial\lambda}\frac{N\left(\sum_{k=0}^m \lambda^k\phi^k\right)}{m!}\bigg|_{\lambda=0} \tag{37}$$

$$\phi^{m+1}(n,t) = \int_0^t d\tau\left(\lim_{\tau\downarrow 0}\int_0^{N_p} d\eta\frac{e^{-(n-\eta)^2/4k(t-\tau)}}{\sqrt{4\pi k(t-\tau)}}A_m(\eta,\tau)\right) \tag{38}$$

Denote

$$\Phi(n,t) := \sum_{m=0}^{\infty}\phi^m(n,t) \tag{39}$$

Then $\Phi(n,t)$ will converge in the short time limit.

Remark 3.7. Unfortunately, I was unsuccessful in finding a proof of convergence for this proposition. In order to do so, one would need to come up with a contraction, and invoke the Banach fixed-point theorem. Hopefully, by the text below, I can make this proposition somewhat plausible.

Listing 2: Maple implementation

```
N := R -> a (diff(R, n$2))^2;
L := R -> diff(R, t$1) - k * diff(R, k$2);
K := exp(-eta^2/(4*k*tau))/sqrt(4*Pi*k*tau);
assume(k>0); assume(a>0);
phi(0) := C*cos(p*Pi*n);
for m from 0 to 5 do;
A(m) := eval(diff(N(sum(phi(k)*lambda^k, k = 0 .. n))/factorial(n), [
    lambda$n]), lambda = 0);
stmnt1 := int(K*subs({n=n-eta, t=t-tau}, A(m)), eta=0..2*Pi);
stmnt2 := limit(stmnt1, tau=0, right)
stmnt3 := int(stmnt2, tau=0..t)
phi(m+1) := simplify(stmnt3);
end do;
```

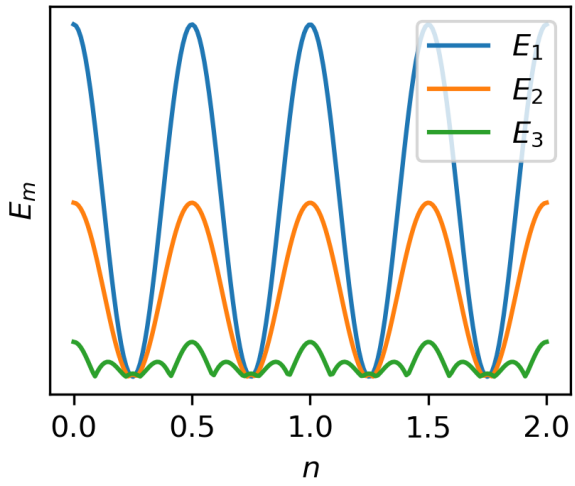

Figure 17: The error $E_m := |L(\sum_{k=0}^{m} \phi^k) - N(\sum_{k=0}^{m} \phi^k)|$. Notice that it seems that $E_m \to 0$ for $m \to \infty$. The constants are taken as; $C = 1$, $a = 0.005$, $p = 2$, $t = 0.01$.

Proposition 3.4. *Consider $\phi_p^0 = c_p \cos(p\pi n)$, with $c_p > 0$ a constant. Then the first coefficient of the Adomian decomposition are given by:*

$$\phi_p^0(n,t) = c_p \cos(p\pi n)$$
$$\phi_p^1(n,t) = \frac{a c_p^2 p^4 \pi^4 t}{2} \cos(p\pi n)^2$$

Remark 3.8. Notice that when $a = 0$, this takes us back to the original Rouse model.

Proof.

$$\begin{aligned} A_0 &= N(\phi_p) = a c_p^2 (p\pi)^4 \cos^2(p\pi n) \\ \phi_p^1 &= K * A_0 \\ &= \int_0^t d\tau \int_0^2 d\eta \frac{e^{-\eta^2/4k\tau}}{\sqrt{4\pi k\tau}} a c_p^2 (p\pi)^4 \cos^2(\pi p(n-\eta)) \end{aligned}$$

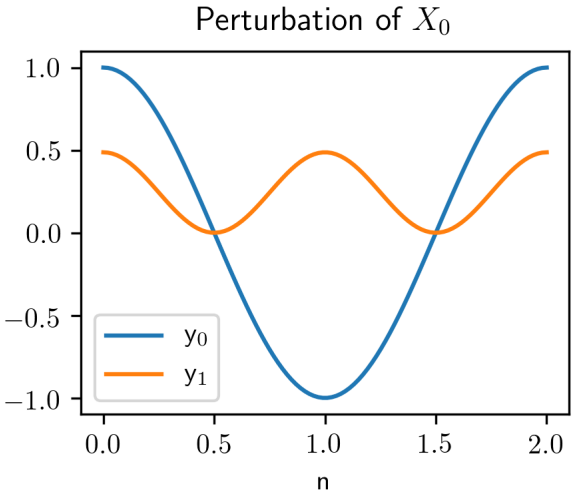

Figure 18: Here you can see the first-order perturbation of the first Rouse mode $X_0 = \cos(\pi n)$.

Considering the inner-most integral, we can do some substitution. Denote $\tilde{\eta} = \eta/\sqrt{4k\tau}$.

$$\begin{aligned} I_{\text{inner}} &:= \int_0^2 d\eta \ \frac{e^{-\eta^2/4k\tau}}{\sqrt{4\pi k\tau}} a c_p^2 (p\pi)^4 \cos^2(\pi p(n-\eta)) \\ &= \int_0^{2/\sqrt{4k\tau}} \sqrt{4k\tau} d\tilde{\eta} \ \frac{e^{-\tilde{\eta}^2}}{\sqrt{4\pi k\tau}} a c_p^2 (p\pi)^4 \cos^2(\pi p(n-\sqrt{4k\tau}\eta)) \\ &= \frac{a c_p^2 (p\pi)^4}{\sqrt{\pi}} \int_0^{2/\sqrt{4k\tau}} d\tilde{\eta} \ \ e^{-\tilde{\eta}^2} \cos^2(\pi p(n-\sqrt{4k\tau}\eta)) \end{aligned}$$

Now we can convert this integral to an error function, see proposition C.1 from the appendix, and the identity $\cos(x)^2 = (1+\sin(2x))/2$.

$$\begin{aligned} I_{\text{inner}} &= \frac{a c_p^2 (p\pi)^4}{\sqrt{\pi}} \int_0^{2/\sqrt{4k\tau}} d\tilde{\eta} \ \ e^{-\tilde{\eta}^2} \frac{1+\sin(2\pi p(n-\sqrt{4k\tau}\eta))}{2} \\ &= \frac{a c_p^2 (p\pi)^4}{\sqrt{\pi}} \left(\frac{\sqrt{\pi}}{4} \text{erf}(2/\sqrt{4k\tau}) + \frac{1}{2} O^{2p\pi n}_{2p\pi\sqrt{4k\tau}}(2/\sqrt{4k\tau}) \right) \end{aligned}$$

Now in order to simplify we consider the short time limit:

$$\lim_{\tau \downarrow 0} I_{\text{inner}} = \frac{a c_p^2 (p\pi)^4}{2\sqrt{\pi}} \left(\frac{1}{2} \text{erf}(\infty) + \frac{1}{2} O_0^{2p\pi n}(\infty) \right)$$

Notice that:

$$\begin{aligned} O_0^{2p\pi n}(\infty) &= \int_0^\infty d\eta e^{-\eta^2} \sin(0\eta + 2p\pi n) \\ &= \sin(2p\pi n) \frac{\sqrt{\pi}}{2} \text{erf}(\infty) \\ &= \sin(2p\pi n) \frac{\sqrt{\pi}}{2} \end{aligned}$$

Evaluating the outer integral now, using the identity

$$\begin{aligned} \phi_p^1 &= \int_0^t d\tau I_{\text{inner}} \\ &= \frac{a c_p^2 (p\pi)^4}{4} \left(1 + \sin(2p\pi n)\right) t \\ &= \frac{a c_p^2 (p\pi)^4 t}{2} \cos(p\pi n)^2 \end{aligned}$$

□

Remark 3.9. At $t = 0$ an arbitrary initial condition can be approximated using finitely many Rouse modes, i.e.

$$\phi(n) = \sum_{p=0}^{P} c_p \phi_p^0 \tag{40}$$

where $\phi_p^0 = X_p = \cos(p\pi n)$ and $c_p = \int_0^2 \phi(n)\phi_p^0 dn$.

Proposition 3.5. *Let $\phi(n)$ be an arbitrary initial condition. The short-term time limit of the semiflexible chainmodel can be approximated by:*

$$\begin{pmatrix} \Phi_1 \\ \vdots \\ \Phi_P \end{pmatrix} = A \begin{pmatrix} \phi_1^0 \\ \vdots \\ \phi_P^0 \end{pmatrix} + \begin{pmatrix} K * \xi_1 \\ \vdots \\ K * \xi_P \end{pmatrix} \tag{41}$$

where $A(t)$ is some matrix containing constants c_p, a, p, π.

Proof. Follows from the fact that the polymer at $t = 0$ can be decomposed in Rouse modes. Then first-order Adomian decomposition can be applied to these individual modes by proposition 3.3, yielding the result. □

4 Conclusion

In summary, the Rouse model and the model of Vanderzande-Vandebroek (in the viscous limit) has been numerically examined. These numerical calculations are inline with the predictions of theory.

Furthermore, a semiflexible chainmodel has been formulated and also numerically been tested. The numerical tests showed that the diffusion σ_{cm} of the semiflexible chainmodel behaved quite similar to the Rouse model and the model of Vanderzande-Vandebroek, depending if active forces were enabled. Also, an analytical analysis of the semiflexible chainmodel has been performed; i.e. a Adomian decomposition scheme giving a short time-limit has been proposed. Unfortunately, the convergence of this scheme has not yet been proven in this thesis. For that, one would have to find a contraction, and apply the Banach-fixed point theorem. Nevertheless, this scheme has, hopefully, been made somewhat plausible.

Once the convergence has been proven, one could derive – analytically – what the short-term statistical properties of the Semiflexible chainmodel are. This inline with the supplemental document supplied by Vanderzande-Vandebroek.

Furthermore, it would be interesting to further investigate how the numerical simulations and the Adomian decomposition match-up in practice for simulating the semiflexible chainmodel. For example; would it be possible to speed-up simulations by applying the Adomian decomposition method instead of time integration?

References

[1] C.W. Gardiner, *Handbook of Stochastic Methods*, Third edition, Springer, ISBN 3-540-20882-8

[2] M. Doi, S.F. Edwards, *The theory of polymer dynamics*, Clarendon Press (Oxford), ISBN 0-19-852033-6.

[3] Hans Vandebroek and Carlo Vanderzande, *Dynamics of a polymer in an active and crowded environment*, arXiv:1507.00889v2

[4] Steven B. Smith, Laura Finzi, Carlos Bustamante. *Direct Mechanical Measurements of the Elasticity of Single DNA Molecules by Using Magnetic Beads*, Science 258 (5085)

[5] John. F. Marko, Eric D. Siggia, *Stretching DNA*, Macromolecules 1995, 28, 8759

[6] Martin Braun. *Differential Equations and Their Applications*, Fourth edition, Springer

[7] C. Vuik, F.J. Vermolen, M.B. van Gijzen, M.J. Vuik. *Numerical methods for ordinary differential equations*, Delft Academic Press, ISBN 9789065623737

[8] Charalambos D. Aliprantis and Owen Burkinshaw, *Principles of real analysis*. Third edition, Academic Press

[9] Dorothee Frey, *Lecture notes Fourier Analysis*. TU Delft (2017)[2]

[10] A.W.C. Lau, A. Davies, J.C. Crocker, T.C. Lubensky, *Microrheology, Stress fluctuations, and Active Behavior of Living Cells*, Physical review letters, DOI: 10.1103/PhysRevLett.91.198101

[11] Sennur Somali, Guzin Gokmen, *Adomian decomposition method for nonlinear Sturm-Liouville problems*, Surveys in Mathematics and its Applications, ISSN 1842-6298

[12] K.K. Kataria, P. Vellaisamy, *Simple parametrization methods for generating Adomian polynomials*, Applicable Analysis and Discrete Mathematics, DOI: 10.2298/AADM160123001K

[13] Crispin Gardiner, *Stochastic Methods: A Handbook for the Natural and Social Sciences*, Springer, ISBN: 978-3540707127

[2]These lecture notes are largely based on J. Korevaar's lecture notes, which are available online via `https://staff.fnwi.uva.nl/j.korevaar/Foubook.pdf`

Appendices

A Derivation forces from potentials

Remark A.1. These calculations have largely been checked with the numerical simulation program. See polymer::test() from src/angle.cpp in the github repository. This improves confidence in below calculations.

Proposition A.1. *For $n, m, o \in \mathbb{N}$, with $n \neq o$ and $n \neq m$, the following equations hold:*

$$\nabla_n |R_n - R_o| = \frac{R_n - R_o}{|R_n - R_o|} \tag{42}$$

$$\nabla_n \frac{1}{|R_n - R_o|} = -\frac{R_n - R_0}{|R_n - R_o|^3} \tag{43}$$

$$\nabla_n \frac{R_n \cdot R_m}{|R_n - R_o|} = \frac{R_m}{|R_n - R_o|} - R_n \cdot R_m \cdot \frac{R_n - R_0}{|R_n - R_o|^3} \tag{44}$$

$$\nabla_n \frac{R_n \cdot R_n}{|R_n - R_o|} = \frac{2R_n}{|R_n - R_o|} - R_n \cdot R_n \frac{R_n - R_o}{|R_n - R_o|^3} \tag{45}$$

$$\begin{aligned} \nabla_n \frac{R_n \cdot R_m}{|R_n - R_m| \cdot |R_n - R_o|} = \frac{R_m}{|R_n - R_m| \cdot |R_n - R_o|} - R_n \cdot R_m \frac{R_n - R_m}{|R_n - R_m|^3 \cdot |R_n - R_o|} \\ - R_n \cdot R_m \frac{R_n - R_o}{|R_n - R_m| \cdot |R_n - R_o|^3} \end{aligned} \tag{46}$$

$$\begin{aligned} \nabla_n \frac{R_n \cdot R_n}{|R_n - R_m| \cdot |R_n - R_o|} = \frac{2R_n}{|R_n - R_m| \cdot |R_n - R_o|} - R_n \cdot R_n \frac{R_n - R_m}{|R_n - R_m|^3 \cdot |R_n - R_o|} \\ - R_n \cdot R_n \frac{R_n - R_o}{|R_n - R_m| \cdot |R_n - R_o|^3} \end{aligned} \tag{47}$$

$$\nabla_n \frac{1}{|R_n - R_m| \cdot |R_n - R_o|} = \frac{R_m - R_n}{|R_n - R_m|^3 \cdot |R_o - R_n|} + \frac{R_o - R_n}{|R_n - R_m| \cdot |R_n - R_o|^3} \tag{48}$$

Proof. Starting with (42);

$$\begin{aligned} \nabla_n |R_n - R_o| &= \frac{\partial}{\partial x_n} \sqrt{(x_n - x_o)^2 + (y_n - y_o)^2 + (z_n - z_o)^2} \hat{x} + ... \hat{y} + ... \hat{z} \\ &= \frac{x_n - x_o}{\sqrt{(x_n - x_o)^2 + (y_n - y_o)^2 + (z_n - z_o)^2}} \hat{x} + ... \hat{y} + ... \hat{z} \\ &= \frac{R_n - R_o}{|R_n - R_o|} \end{aligned}$$

Starting with (43), we use the chain rule:

$$\nabla_n \frac{1}{|R_n - R_o|} = -\frac{1}{|R_n - R_o|^2} \nabla_n |R_n - R_o|$$

Substituting (42) gives (43).

Now for (44), we use the quotient rule of the divergence:

$$\nabla_n \frac{R_n \cdot R_m}{|R_n - R_o|} = \frac{(\nabla_n R_n \cdot R_m) \cdot |R_n - R_o| - R_n \cdot R_m \cdot (\nabla_n |R_n - R_o|)}{|R_n - R_o|^2}$$

Now we have to find the two individual divergences in the above equation:

$$\begin{aligned}\nabla_n R_n \cdot R_m &= \frac{\partial}{\partial x_n}(x_n x_m + y_n y_m + z_n z_m)\hat{x} + ...\hat{y} + ...\hat{z} \\ &= x_m\hat{x} + y_m\hat{y} + z_m\hat{z} \\ &= R_m\end{aligned}$$

Substituting back gives (44).

Now (45). Again applying the quotient rule:

$$\nabla_n \frac{R_n \cdot R_n}{|R_n - R_o|} = \frac{(\nabla_n R_n \cdot R_n)|R_n - R_o| - R_n \cdot R_n \cdot (\nabla_n |R_n - R_o|)}{|R_n - R_o|^2}$$

Now only one divergence identity is missing:

$$\nabla_n R_n \cdot R_n = \frac{\partial}{\partial x_n}(x_n^2 + y_n^2 + z_n^2)\hat{x} + ...\hat{y} + ...\hat{z} = 2x_n\hat{x} + 2y_n\hat{y} + 2z_n\hat{z} = 2R_n$$

Substituting this gives (45).

Now (46). Once again applying the quotient rule:

$$\begin{aligned}\nabla_n \frac{R_n \cdot R_m}{|R_n - R_m| \cdot |R_n - R_o|} &= \frac{(\nabla_n R_n \cdot R_m) \cdot |R_n - R_m| \cdot |R_n - R_o|}{|R_n - R_m|^2 \cdot |R_n - R_o|^2} \\ &- \frac{R_n \cdot R_m \cdot (\nabla_n |R_n - R_m| \cdot |R_n - R_o|)}{|R_n - R_m|^2 \cdot |R_n - R_o|^2} \\ &= \frac{R_m}{|R_n - R_m| \cdot |R_n - R_o|} \\ &- R_n \cdot R_m \frac{(\nabla_n |R_n - R_m|) \cdot |R_n - R_o| + |R_n - R_m| \cdot (\nabla_n |R_n - R_o|)}{|R_n - R_m|^2 \cdot |R_n - R_o|^2} \\ &= \frac{R_m}{|R_n - R_m| \cdot |R_n - R_o|} - R_n \cdot R_m \frac{R_n - R_m}{|R_n - R_m|^3 \cdot |R_n - R_o|} \\ &- R_n \cdot R_m \frac{R_n - R_o}{|R_n - R_m| \cdot |R_n - R_o|^3}\end{aligned}$$

And hereby the identity is proven.

Now (47). Applying the quotient rule:

$$\begin{aligned}\nabla_n \frac{R_n \cdot R_n}{|R_n - R_m| \cdot |R_n - R_o|} &= \frac{(\nabla_n R_n \cdot R_n) \cdot |R_n - R_m| \cdot |R_n - R_o|}{|R_n - R_m|^2 \cdot |R_n - R_o|^2} \\ &- R_n \cdot R_n \frac{\nabla_n |R_n - R_m| \cdot |R_n - R_o|}{|R_n - R_m|^2 \cdot |R_n - R_o|^2} \\ &= \frac{2R_n}{|R_n - R_m| \cdot |R_n - R_o|} - R_n \cdot R_n \frac{R_n - R_m}{|R_n - R_m|^3 \cdot |R_n - R_o|} \\ &- R_n \cdot R_n \frac{R_n - R_o}{|R_n - R_m| \cdot |R_n - R_o|^3}\end{aligned}$$

Now (48). Applying the chain rule:

$$\begin{aligned}\nabla_n \frac{1}{|R_n - R_m| \cdot |R_n - R_o|} = \\ \frac{-1}{|R_n - R_m|^2 \cdot |R_n - R_o|^2} \cdot \left(\frac{R_n - R_m}{|R_n - R_m|} \cdot |R_n - R_o| + |R_n - R_m| \cdot \frac{R_n - R_o}{|R_n - R_o|} \right) = \\ \frac{R_m - R_n}{|R_n - R_m|^3 \cdot |R_o - R_n|} + \frac{R_o - R_n}{|R_n - R_m| \cdot |R_n - R_o|^3}\end{aligned}$$

And this is the proof of the last identity, completing the proof. □

Spring force

The vector associated with the i-th spring is notated by l_i. Here $|l_i| = l$ for all i. In other words; the length of all the springs is constant when no forces act on it. Also, l_i and $(R_i - R_{i+1})$ point in the same direction such that:

$$\frac{l_i \cdot (R_i - R_{i+1})}{|l_i| \cdot |R_i - R_{i+1}|} = 1$$

Now we can explicitly define l_i;

$$l_i := l \frac{R_i - R_{i+1}}{|R_i - R_{i+1}|} \tag{49}$$

Let's first consider the first term of the right hand side of (21). For all the monomers except the first and last ($i \neq 1, N$), the following holds:

$$\nabla_n \left(\frac{k}{2} \sum_{i=1}^{N-1} |R_i - R_{i+1} - l_i|^2 \right) = \frac{k}{2} \nabla_n \left(|R_{n-1} - R_n - l_{n-1}|^2 + |R_n - R_{n+1} - l_n|^2 \right)$$

We may rewrite the two terms on the right hand side in the following way:

$$\begin{aligned}
\nabla_n |R_{n-1} - R_n - l_{n-1}|^2 &= \nabla_n \left| R_{n-1} - R_n - l \frac{R_{n-1} - R_n}{|R_{n-1} - R_n|} \right|^2 \\
&= \nabla_n \left| (R_{n-1} - R_n) \left(1 - \frac{l}{|R_{n-1} - R_n|} \right) \right|^2 \\
&= \nabla_n \left(|R_{n-1} - R_n|^2 \left(1 - \frac{l}{|R_{n-1} - R_n|} \right)^2 \right)
\end{aligned}$$

Using the product rule:

$$\begin{aligned}
\nabla_n |R_{n-1} - R_n - l_{n-1}|^2 &= \left(\nabla_n |R_{n-1} - R_n|^2 \right) \left(1 - \frac{l}{|R_{n-1} - R_n|} \right)^2 \\
&\quad + |R_{n-1} - R_n|^2 \nabla_n \left(1 - \frac{l}{|R_{n-1} - R_n|} \right)^2 \\
&= 2 |R_{n-1} - R_n| \left(\nabla_n |(R_{n-1} - R_n)| \right) \left(1 - \frac{l}{|R_{n-1} - R_n|} \right)^2 \\
&\quad + 2 |R_{n-1} - R_n|^2 \left(1 - \frac{l}{|R_{n-1} - R_n|} \right) \nabla_n \left(1 - \frac{l}{|R_{n-1} - R_n|} \right)
\end{aligned}$$

From (42) we know that:

$$\nabla_n |R_{n-1} - R_n| = \frac{R_n - R_{n-1}}{|R_{n-1} - R_n|}$$

And from (43) we know that:

$$\nabla_n \left(1 - \frac{l}{|R_{n-1} - R_n|} \right) = \nabla_n \frac{-l}{|R_{n-1} - R_n|} = l \frac{R_n - R_{n-1}}{|R_{n-1} - R_n|^3}$$

Substituting gives:

$$\begin{aligned}\nabla_n|R_{n-1}-R_n-l_{n-1}|^2 &= 2|R_{n-1}-R_n|\frac{R_n-R_{n-1}}{|R_{n-1}-R_n|}\left(1-\frac{l}{|R_{n-1}-R_n|}\right)^2\\ &+2|R_{n-1}-R_n|^2\left(1-\frac{l}{|R_{n-1}-R_n|}\right)l\frac{R_n-R_{n-1}}{|R_{n-1}-R_n|^3}\\ &=2(R_n-R_{n-1})\left(1-\frac{l}{|R_{n-1}-R_n|}\right)^2\\ &+2l\left(1-\frac{l}{|R_{n-1}-R_n|}\right)\frac{R_n-R_{n-1}}{|R_{n-1}-R_n|}\\ &=2(R_n-R_{n-1})\left(1-\frac{l}{|R_{n-1}-R_n|}\right)\end{aligned}$$

Likewise:

$$\nabla_n|R_n-R_{n+1}-l_n|^2=2(R_n-R_{n+1})\left(1-\frac{l}{|R_{n+1}-R_n|}\right)$$

Finally:

$$\begin{aligned}\nabla_n\left(\frac{k}{2}\sum_{i=1}^{N-1}|R_i-R_{i+1}-l_i|^2\right) &= k(R_n-R_{n-1})\left(1-\frac{l}{|R_{n-1}-R_n|}\right)\\ &+k(R_n-R_{n+1})\left(1-\frac{l}{|R_{n+1}-R_n|}\right)\end{aligned}\quad(50)$$

And notice if $l=0$ this reduces to the familiar equation:

$$\nabla_n\left(\frac{k}{2}\sum_{i=1}^{N-1}|R_i-R_{i+1}-l_i|^2\right)=k\cdot(2R_n-R_{n-1}-R_{n+1})\quad(51)$$

Angle force

Now let's consider the second part of equation (21). Notice that the particle R_n only occurs in u_n and u_{n+1};

$$\begin{aligned}&\vdots\\ u_{n-1}&=R_{n-1}-R_{n-2}\\ u_n&=R_n-R_{n-1}\\ u_{n+1}&=R_{n+1}-R_n\\ u_{n+2}&=R_{n+2}-R_{n+1}\\ &\vdots\end{aligned}$$

Therefore R_n only occurs in $\theta_n,\theta_{n+1},\theta_{n+2}$. In other words; all the other angles are not a function of R_n. This is important to realize because this simplifies calculating F_n greatly; for all the monomers except the first and last monomer[3] the following holds:

$$\begin{aligned}\nabla_n\left(\frac{a}{2}\sum_{i=1}^{N-2}\left(1-\frac{u_i\cdot u_{i+1}}{|u_i|\cdot|u_{i+1}|}\right)^2\right) &= \frac{a}{2}\nabla_n\left(1-\frac{u_{n+1}\cdot u_{n+2}}{|u_{n+1}|\cdot|u_{n+2}|}\right)^2\\ &+\frac{a}{2}\nabla_n\left(1-\frac{u_n\cdot u_{n+1}}{|u_n|\cdot|u_{n+1}|}\right)^2\\ &+\frac{a}{2}\nabla_n\left(1-\frac{u_{n-1}\cdot u_n}{|u_{n-1}|\cdot|u_n|}\right)^2\end{aligned}$$

[3]Since θ_1 and θ_N don't exists, also $\nabla_1(1-\cos\theta_1)^2$ and $\nabla_N(1-\cos\theta_N)^2$ don't exist.

We define:

$$F_n^-(u_{n-1},u_n) := \nabla_n\left(1-\frac{u_n\cdot u_{n-1}}{|u_n|\cdot|u_{n-1}|}\right)$$
$$F_n^0(u_n,u_{n+1}) := \nabla_n\left(1-\frac{u_{n+1}\cdot u_n}{|u_{n+1}|\cdot|u_n|}\right)$$
$$F_n^+(u_{n+1},u_{n+2}) := \nabla_n\left(1-\frac{u_{n+2}\cdot u_{n+1}}{|u_{n+2}|\cdot|u_{n+1}|}\right)$$

Notice that because of the chain rule we can simplify things a bit further:

$$\frac{a}{2}\nabla_n\left(1-\frac{u_n\cdot u_{n-1}}{|u_n|\cdot|u_{n-1}|}\right)^2 = a(1-\cos\theta_{n-1})F_n^-(u_{n-1},u_n) \tag{52}$$
$$\frac{a}{2}\nabla_n\left(1-\frac{u_{n+1}\cdot u_n}{|u_{n+1}|\cdot|u_n|}\right)^2 = a(1-\cos\theta_n)F_n^0(u_n,u_{n+1}) \tag{53}$$
$$\frac{a}{2}\nabla_n\left(1-\frac{u_{n+2}\cdot u_{n+1}}{|u_{n+2}|\cdot|u_{n+1}|}\right)^2 = a(1-\cos\theta_{n+1})F_n^+(u_{n+1},u_{n+2}) \tag{54}$$

Now we want to describe the above equations in terms of the positions $\{R_n\}_{n=1}^N$. In order to do this I present the following proposition.

Applying the proposition

No we can write out F_n^-, F_n^0, F_n^+ as a function of the positions $\{R_n\}_{n=1}^N$.

Finding an expression for F_n^-

$$\begin{aligned}F_n^-(R_{n-2},R_{n-1},R_n) &= \nabla_n\left(1-\frac{(R_{n-1}-R_{n-2})\cdot(R_n-R_{n-1})}{|R_{n-1}-R_{n-2}|\cdot|R_n-R_{n-1}|}\right)\\ &= \nabla_n\left(1-\frac{R_{n-1}\cdot R_n - R_{n-1}\cdot R_{n-1} - R_{n-2}\cdot R_n + R_{n-2}\cdot R_{n-1}}{|R_{n-1}-R_{n-2}|\cdot|R_n-R_{n-1}|}\right)\\ &= \nabla_n\left(\frac{R_{n-1}\cdot R_{n-1} + R_{n-2}\cdot R_n - R_{n-2}\cdot R_{n-1} - R_{n-1}\cdot R_n}{|R_{n-1}-R_{n-2}|\cdot|R_n-R_{n-1}|}\right)\end{aligned}$$

Because of the proposition we have:

$$\nabla_n\frac{R_{n-1}\cdot R_{n-1}-R_{n-2}\cdot R_{n-1}}{|R_n-R_{n-1}|} = (R_{n-1}\cdot R_{n-1}-R_{n-2}\cdot R_{n-1})\frac{R_{n-1}-R_n}{|R_n-R_{n-1}|^3}$$
$$\nabla_n\frac{(R_{n-2}-R_{n-1})\cdot R_n\cdot R_n}{|R_n-R_{n-1}|} = \frac{R_{n-2}-R_{n-1}}{|R_n-R_{n-1}|} + (R_{n-2}-R_{n-1})\cdot R_n\frac{R_{n-1}-R_n}{|R_n-R_{n-1}|^3}$$

Substituting this back gives:

$$\begin{aligned}|R_{n-1}-R_{n-2}|F_n^-(R_{n-2},R_{n-1},R_n) &= (R_{n-1}\cdot R_{n-1}-R_{n-2}\cdot R_{n-1})\frac{R_{n-1}-R_n}{|R_n-R_{n-1}|^3}\\ &+ \frac{R_{n-2}-R_{n-1}}{|R_n-R_{n-1}|} + (R_{n-2}-R_{n-1})\cdot R_n\frac{R_{n-1}-R_n}{|R_n-R_{n-1}|^3}\end{aligned} \tag{55}$$

Rewriting a bit:

$$\begin{aligned}|R_{n-1}-R_{n-2}|\cdot|R_n-R_{n-1}|\cdot F_n^-(R_{n-2},R_{n-1},R_n) &= R_{n-2}-R_{n-1}\\ &+ (R_{n-1}\cdot R_{n-1}-R_{n-2}\cdot R_{n-1}+(R_{n-2}-R_{n-1})\cdot R_n)\frac{R_{n-1}-R_n}{|R_n-R_{n-1}|^2}\end{aligned}$$

Now using the geometric interpretation (20) this simplifies to:

$$|u_{n-1}| \cdot |u_n| \cdot F_n^-(R_{n-2}, R_{n-1}, R_n) = R_{n-2} - R_{n-1} + (-u_{n-1} \cdot u_n) \frac{R_{n-1} - R_n}{|R_n - R_{n-1}|^2}$$

Finally:

$$F_n^-(R_{n-2}, R_{n-1}, R_n) = \frac{R_{n-2} - R_{n-1}}{|u_{n-1}| \cdot |u_n|} - \cos(\theta_{n-1}) \frac{R_{n-1} - R_n}{|R_n - R_{n-1}|^2} \tag{56}$$

Finding an expression for F_n^+

We also rewrite F_n^+ in terms of R_{n+2}, R_{n+1}, R_n:

$$F_n^+(R_n, R_{n+1}, R_{n+2}) = \nabla_n \left(1 - \frac{(R_{n+1} - R_n) \cdot (R_{n+2} - R_{n+1})}{|R_n - R_{n+1}| \cdot |R_{n+2} - R_{n+1}|}\right)$$

Now without further deriving, we note the following symmetry between F_n^- and F_n^+:

$$F_n^+(R_n, R_{n+1}, R_{n+2}) = F_n^-(R_{n+2}, R_{n+1}, R_n) \tag{57}$$

Finding an expression for F_n^0

Now we determine F_n^0:

$$\begin{aligned}
F_n^0(R_{n-1}, R_n, R_{n+1}) &= \nabla_n \left(1 - \frac{(R_n - R_{n-1}) \cdot (R_{n+1} - R_n)}{|R_n - R_{n-1}| \cdot |R_n - R_{n+1}|}\right) \\
&= \nabla_n \left(1 - \frac{R_n \cdot R_{n+1} - R_n \cdot R_n - R_{n-1} \cdot R_{n+1} + R_{n-1} \cdot R_n}{|R_n - R_{n-1}| \cdot |R_n - R_{n+1}|}\right) \\
&= \nabla_n \left(\frac{R_n \cdot R_n + R_{n-1} \cdot R_{n+1} - R_n \cdot R_{n+1} - R_{n-1} \cdot R_n}{|R_n - R_{n-1}| \cdot |R_n - R_{n+1}|}\right)
\end{aligned}$$

Using the above proposition:

$$\begin{aligned}
\nabla_n \frac{R_n \cdot R_n}{|R_n - R_{n-1}| \cdot |R_n - R_{n+1}|} &= \frac{2R_n}{|R_n - R_{n-1}| \cdot |R_n - R_{n+1}|} \\
&\quad + R_n \cdot R_n \frac{R_{n-1} - R_n}{|R_n - R_{n-1}|^3 \cdot |R_n - R_{n+1}|} \\
&\quad + R_n \cdot R_n \frac{R_{n+1} - R_n}{|R_n - R_{n-1}| \cdot |R_n - R_{n+1}|^3} \\
\nabla_n \frac{R_{n-1} \cdot R_{n+1}}{|R_n - R_{n-1}| \cdot |R_n - R_{n+1}|} &= (R_{n-1} \cdot R_{n+1}) \frac{R_{n-1} - R_n}{|R_n - R_{n-1}|^3 \cdot |R_n - R_{n+1}|} \\
&\quad + (R_{n-1} \cdot R_{n+1}) \frac{R_{n+1} - R_n}{|R_n - R_{n-1}| \cdot |R_n - R_{n+1}|^3} \\
\nabla_n \frac{-R_n \cdot (R_{n+1} + R_{n-1})}{|R_n - R_{n-1}| \cdot |R_n - R_{n+1}|} &= -\frac{R_{n-1} + R_{n+1}}{|R_n - R_{n-1}| \cdot |R_n - R_{n+1}|} \\
&\quad + R_n \cdot (R_{n-1} + R_{n+1}) \frac{R_n - R_{n-1}}{|R_n - R_{n-1}|^3 \cdot |R_n - R_{n+1}|} \\
&\quad + R_n \cdot (R_{n-1} + R_{n+1}) \frac{R_n - R_{n+1}}{|R_n - R_{n-1}| \cdot |R_n - R_{n+1}|^3}
\end{aligned}$$

This gives:

$$\begin{aligned}
&|R_n - R_{n-1}| \cdot |R_n - R_{n+1}| \cdot F_n^0(R_{n-1}, R_n, R_{n+1}) = 2R_n - R_{n-1} - R_{n+1} \\
&+ \left(\frac{R_{n+1} - R_n}{|R_n - R_{n+1}|^2} + \frac{R_{n-1} - R_n}{|R_n - R_{n-1}|^2}\right) [R_{n-1} \cdot R_{n+1} + R_n \cdot R_n - R_n \cdot (R_{n-1} + R_{n+1})]
\end{aligned} \tag{58}$$

Using the geometric interpretation (20) this simplifies to:

$$|u_n| \cdot |u_{n+1}| \cdot F_n^0(R_{n-1}, R_n, R_{n+1}) = 2R_n - R_{n-1} - R_{n+1} + \left(\frac{R_{n+1} - R_n}{|u_{n+1}|^2} + \frac{R_{n-1} - R_n}{|u_n|^2} \right) [-u_n \cdot u_{n+1}]$$

Which is:

$$F_n^0(R_{n-1}, R_n, R_{n+1}) = 2R_n - R_{n-1} - R_{n+1} - \left(\frac{R_{n+1} - R_n}{|R_n - R_{n+1}|^2} + \frac{R_{n-1} - R_n}{|R_n - R_{n-1}|^2} \right) \cos(\theta_n) \tag{59}$$

Explicit expression angle force

So this leads up to an expression for $F_{\text{angle},n}$ as an explicit function of the particles $\{R_n(t)\}_{n=1}^N\}$. For almost all of the particles ($n \neq 1, 2, N-1, N$) we have:

$$\begin{aligned} -F_{\text{angle},n} &= a \cdot (1 - \cos\theta_{n-1}) \cdot F_n^{-1} \\ &+ a \cdot (1 - \cos\theta_n) \cdot F_n^0 \\ &+ a \cdot (1 - \cos\theta_{n+1}) \cdot F_n^{+1} \end{aligned}$$

The forces for the remaining particles are given by:

$$\begin{aligned} -F_{\text{angle},1} &= a \cdot (1 - \cos\theta_2) \cdot F_n^{+1} \\ -F_{\text{angle},2} &= +a \cdot (1 - \cos\theta_2) \cdot F_n^0 + a \cdot (1 - \cos\theta_3) \cdot F_n^{+1} \\ -F_{\text{angle},N-1} &= a \cdot (1 - \cos\theta_{N-2}) \cdot F_n^{-1} + a \cdot (1 - \cos\theta_N - 1) \cdot F_n^0 \\ -F_{\text{angle},N} &= a \cdot (1 - \cos\theta_N - 1) \cdot F_n^{-1} \end{aligned}$$

Substituting gives:

$$\begin{aligned} -F_{\text{angle},n} &= a \cdot (1 - \cos\theta_{n-1}) \cdot \left(R_{n-2} - R_{n-1} - \cos(\theta_{n-1}) \frac{R_{n-1} - R_n}{|R_n - R_{n-1}|^2} \right) \\ &+ a \cdot (1 - \cos\theta_n) \cdot \left(2R_n - R_{n-1} - R_{n+1} - \left(\frac{R_{n+1} - R_n}{|R_n - R_{n+1}|^2} + \frac{R_{n-1} - R_n}{|R_n - R_{n-1}|^2} \right) \cos(\theta_n) \right) \\ &+ a \cdot (1 - \cos\theta_{n+1}) \cdot \left(R_{n+2} - R_{n+1} - \cos(\theta_{n+1}) \frac{R_{n+1} - R_n}{|R_n - R_{n+1}|^2} \right) \end{aligned}$$

Expressing in complex coefficients, and using the identity; $1 - \cos(x) = 2\sin^2(x/2)$:

$$\begin{aligned} \frac{-F_{\text{angle},n}}{2a} &= \sin(\theta_{n-1}/2) \cdot \left(R_{n-2} - R_{n-1} - \cos(\theta_{n-1}) \frac{R_{n-1} - R_n}{|R_n - R_{n-1}|^2} \right) \\ &+ \sin(\theta_n/2) \cdot \left(2R_n - R_{n-1} - R_{n+1} - \left(\frac{R_{n+1} - R_n}{|R_n - R_{n+1}|^2} + \frac{R_{n-1} - R_n}{|R_n - R_{n-1}|^2} \right) \cos(\theta_n) \right) \\ &+ \sin(\theta_{n+1}/2) \cdot \left(R_{n+2} - R_{n+1} - \cos(\theta_{n+1}) \frac{R_{n+1} - R_n}{|R_n - R_{n+1}|^2} \right) \end{aligned} \tag{60}$$

B Derivation of the Rouse Modes

This derivation is inspired by Doi M, Edwards S.F. The theory of Polymer Dynamics (Oxford 1994) Appendix 4.II. The main difference is that they derive the Rouse Modes for when n is a continuous variable in $[0, N_p - 1]$. In this document only discrete n is used, i.e. $n \in \{0, 1, ..., N_p - 1\}$.

Lemma B.1 (Summation by parts)**.** *Let $\{a_n\}_{n\geq 1}$ and $\{b_n\}_{n\geq 1}$ be two sequences in $\mathbb{R}$. And let $A_n = \sum_{i=1}^{n} a_i$, then the following identity holds:*

$$\sum_{n=j+1}^{k} a_n b_n = \sum_{n=j}^{k-1} A_n(b_n - b_{n+1}) + A_k b_k - A_j b_j, \quad k > j \tag{61}$$

In particular, for $j = 0$

$$\sum_{n=1}^{k} a_n b_n = \sum_{n=1}^{k-1} A_n(b_n - b_{n+1}) + A_k b_k \tag{62}$$

Proof. Notice that $A_{n+1} - A_n = a_{n+1}$ for all $n \geq 1$ and $A_1 = a_1$.

$$\begin{aligned}
\sum_{n=j+1}^{k} a_n b_n &= \sum_{n=j+1}^{k} (A_n - A_{n-1}) b_n \\
&= \sum_{n=j+1}^{k} A_n b_n - \sum_{n=j+1}^{k} A_{n-1} b_n \\
&= \sum_{n=j+1}^{k} A_n b_n - \sum_{n=j}^{k} A_n b_{n+1} \\
&= \sum_{n=j}^{k-1} A_n(b_n - b_{n+1}) + A_k b_k - A_j b_j
\end{aligned}$$

This holds only of course when $j < k$. And if we hold to convention $\sum_{x\in\emptyset} x = 0$ then the case for $j = 0$ immediately follows. □

Remark B.1. Notice that this is similar with the well known integration by parts formula $\int fG = FG| - \int fG$ in the sense that $a_n \cong f$ and $b_n \cong G$. Furthermore, the summation by parts lemma is sometimes called Abel's lemma.

Definition B.1. The first numerical derivative of R_n is denoted by ΔR_n and given by:

$$\Delta R_n = R_{n+1} - R_n \tag{63}$$

The second order numerical derivate of

Theorem B.1. *Let $I = \{0, 1, ..., N-1\}$ and $\{x_i\}_{i\in I}$ be a sequence in $\mathbb{R}$. Then there exists a linear transform $X : \{x_i\}_{i\in I} \times I \to \{X_p\}_{p\in I}$, denoted by $X_p = X[x_n]^p$, such that the rouse model (17) can be transformed and characterized by the following form*

$$\frac{\partial}{\partial t} X[R_n]^p = -k_p X[R_n]^p + X[\xi_n]^p, \quad k_p > 0 \tag{64}$$

Proof. Consider the following linear transformation:

$$X_p = \frac{1}{N_p 2} \sum_{n=0}^{N_p-1} R_n c_n^p \tag{65}$$

We'll try to find expressions for c_n^p in order to transform the rouse model

$$\frac{\partial R_n}{\partial t} = -k(2R_n - R_{n-1} - R_{n+1}) + \xi_n \tag{66}$$

to the following form

$$\frac{\partial X_p}{\partial t} = -k_p X_p + \xi_p \tag{67}$$

We need to introduce a few boundary conditions in order to make sense of the first- and second-order numerical derivatives[4]

$$R_{-1} = R_0, \;\; R_N = R_{N-1}, \;\; R_{-2} = -R_{-1}, \;\; R_{N+1} = -R_N \tag{68}$$

Notice that these boundary conditions are also known as 'phantom beads'. Substitution gives

$$\frac{1}{N}\sum_{n=0}^{N_p-1} \frac{\partial R_n}{\partial t} c_n^p = \frac{1}{N}\sum_{n=0}^{N_p-1} \left[-k(2R_n - R_{n+1} - R_{n-1}) + \xi_n)\right] c_n^p$$

Now applying summation by parts

$$\begin{aligned}\sum_{n=0}^{N_p-1} -k(2R_n - R_{n+1} - R_{n-1})c_n^p &= \sum_{n=0}^{N_p-1} -k(R_n - R_{n+1}) \cdot (c_n^p - c_{n+1}^p) \\ &\quad -k(R_n - R_{n+1}) \cdot c_n^p|_{n=-1}^{N_p-1} \\ &= \sum_{n=0}^{N_p-1} -k(R_n - R_{n+1}) \cdot (c_n^p - c_{n+1}^p)\end{aligned}$$

In above equation the boundary terms disappeared due to the phantom beads of the Rouse model $R_0 = R_{-1}$ and $R_{N_p-1} = R_{N_p}$. Doing summation by parts a second time will give:

$$\begin{aligned}\sum_{n=0}^{N_p-1} -k(R_n - R_{n+1}) \cdot (c_n^p - c_{n+1}^p) &= -kR_n(c_n^p - c_{n+1}^p)\big|_{n=-1}^{N_p-1} \\ &\quad + \sum_{n=0}^{N_p-1} -kR_n \cdot (2c_n^p - c_{n+1}^p - c_{n-1}^p)\end{aligned}$$

Therefore we have conditions for c_n^p

$$\begin{cases} k(2c_n^p - c_{n+1}^p - c_{n-1}^p) = -k_p c_n^p \\ c_0^p - c_{-1}^p = 0 \\ c_{N_p}^p - c_{N_p-1}^p = 0 \end{cases} \tag{69}$$

This has the well known solution:

$$c_n^p = \cos\left(\frac{\pi p(n+1/2)}{N}\right) \tag{70}$$

$$2\cos\left(\frac{\pi p(n+1/2)}{N}\right) - \cos\left(\frac{\pi p(n+3/2)}{N}\right) - \cos\left(\frac{\pi p(n-1/2)}{N}\right) = \frac{k_p}{k}\cos\left(\frac{\pi p(n+1/2)}{N}\right)$$

Notice, by the identity $\cos(x) - \cos(y) = -2\sin(x/2 + y/2)\sin(x/2 - y/2)$, we have

$$\begin{aligned}\cos\left(\frac{\pi p(n+1/2)}{N}\right) - \cos\left(\frac{\pi p(n+3/2)}{N}\right) &= 2\sin\left(\frac{\pi p(n+1)}{N}\right)\sin\left(\frac{\pi p}{2N}\right) \\ \cos\left(\frac{\pi p(n+1/2)}{N}\right) - \cos\left(\frac{\pi p(n-1/2)}{N}\right) &= -2\sin\left(\frac{\pi pn}{N}\right)\sin\left(\frac{\pi p}{2N}\right)\end{aligned}$$

[4] I.e. $R_{n+1} - R_n$ can be seen as a first order derivative and $2R_n - R_{n+1} - R_{n-1}$ can be seen as a second order derivative.

Therefore:

$$\begin{aligned}\frac{k_p}{k}\cos\left(\frac{\pi p(n+1/2)}{N}\right) &= 2\left(\sin\left(\frac{\pi p(n+1)}{N}\right)-\sin\left(\frac{\pi pn}{N}\right)\right)\sin\left(\frac{\pi p}{2N}\right)\\ &= 4\cos\left(\frac{\pi p(n+1/2)}{N}\right)\left(\sin\frac{\pi p}{2N}\right)^2\\ \implies k_p &= 4k\sin^2\left(\frac{\pi p}{2N}\right)\end{aligned}$$

It makes sense at this point to take $\xi_p = \frac{1}{N}\sum_{n=0}^{N_p-1}\xi_n c_n^p$. Conclusion: the □

Remark B.2. The inverse transform is given by

$$X^{-1}\left[X_p\right] = \sum_{p<|N_p|} X_p c_n^p = X_0 + 2\sum_{p=1}^{N_p-1} X_p c_n^p \tag{71}$$

Remark B.3. We see that the eigenfunctions we found are all cosine-functions. Therefore the Rouse modes can be seen as a Fourier series transform from $n \to p$.

Notice that it's slightly easier to derive k_p using properties of Fourier series transform. I.e. let $\mathcal{F}[\cdot]$ be the Fourier series transform given by $\mathcal{F}[f(n)](\omega) = \sum_{n\in\mathbb{Z}} f(n)e^{-i\omega n}$, then $\mathcal{F}[f(n-n_o)] = e^{-in_0\omega}\mathcal{F}[f(n)]$. It follows that

$$\begin{aligned}\frac{\partial\mathcal{F}\left[R_n\right]}{\partial t} &= -k(1-e^{i\omega}+1-e^{i\omega})\mathcal{F}\left[R_n\right]+\mathcal{F}\left[\xi_n\right]\\ &= -k(2-2\cos(\omega/2))\mathcal{F}\left[R_n\right]+\mathcal{F}\left[\xi_n\right]\\ &= -4k\sin^2(\omega/2)\mathcal{F}\left[R_n\right]+\mathcal{F}\left[\xi_n\right]\end{aligned}$$

Showing that indeed $k_p = 4k\sin^2\left(\pi p/2N\right)$.

Proposition B.1. *The Rouse transform of the stochastic force $\xi_n(t)$ characterized by*

$$\begin{aligned}\langle\xi_n(t)\rangle &= 0\\ \langle\xi_n(t)\cdot\xi_m(t+\tau)\rangle &= \delta_{n,m}Ce^{-\tau/\tau_A}\end{aligned}$$

is given by

$$\begin{aligned}\langle\xi_p\rangle &= 0\\ \langle\xi_p(t)\cdot\xi_q(t+\tau)\rangle &= \delta_{p,q}Ce^{-\tau/\tau_A}\end{aligned}$$

Proof. The first moment:

$$\langle\xi_p\rangle = \int_0^N \langle\xi_n(t)\rangle\cos\left(\frac{p\pi n}{N}\right)dn = 0$$

The second moment, we use the 2D Rouse transform similar to the 2D Fourier transform:

$$\begin{aligned}\langle\xi_p(t)\cdot\xi_q(t+\tau)\rangle &= \int_0^N dn\int_0^N dm\;\delta_{n,m}\cos\left(\frac{p\pi n}{N}\right)\cos\left(\frac{q\pi m}{N}\right)Ce^{-\tau/\tau_A}\\ &= Ce^{-\tau/\tau_A}\int_0^N dn\;\cos\left(\frac{p\pi n}{N}\right)\cos\left(\frac{q\pi n}{N}\right)\\ &= Ce^{-\tau/\tau_A}\int_0^N dn\frac{1}{2}\left(\cos\left(\frac{(p+q)\pi n}{N}\right)+\cos\left(\frac{(p-q)\pi n}{N}\right)\right)\\ &= \frac{Ce^{-\tau/\tau_A}}{2}\left[\frac{N}{(p+q)\pi}\sin\left(\frac{(p+q)\pi n}{N}\right)+\frac{N}{(p-q)\pi}\sin\left(\frac{(p-q)\pi n}{N}\right)\right]_0^N\\ &= \frac{Ce^{-\tau/\tau_A}}{2}\left[\frac{N}{(p-q)\pi}\sin\left(\frac{(p-q)\pi n}{N}\right)\right]_0^N\end{aligned}$$

Now using the identity $\sin(x)/x \to 1$ when $x \to 0$ gives:

$$\begin{aligned}\langle \xi_p(t) \cdot \xi_q(t+\tau) \rangle &= \frac{Ce^{-\tau/\tau_A}}{2} 2 \left[\frac{\sin(x)}{x} \right]_{x=0} \\ &= \delta_{p,q} Ce^{-\tau/\tau_A}\end{aligned}$$

□

C Gaussian integral with complex argument

The motivation for this appendix is to evaluate integrals such as

$$\int_0^n d\eta e^{-\eta^2}\cos(C\eta)$$

in terms of error functions.

Definition C.1. The error function is defined as:

$$\operatorname{erf}(x) = \frac{1}{\sqrt{\pi}}\int_{-x}^{x} e^{-t^2}dt = \frac{2}{\sqrt{\pi}}\int_0^x e^{-t^2}dt$$

Remark C.1. Recall the following important properties of error functions:

- $\operatorname{erf}(r) = -\operatorname{erf}(-r)$ for any $r \in \mathbb{R}$, since the Gaussian is an even function.
- $\operatorname{erf}(\bar{z}) = \overline{\operatorname{erf}(z)}$ for any $z \in \mathbb{C}$
- $\lim_{r\to\pm\infty}\operatorname{erf}(r) = \pm 1$

Proposition C.1.

$$\int_0^n d\eta e^{-\eta^2}\cos(C\eta) = \frac{\sqrt{\pi}e^{-C^2/4}}{4}(erf(n+iC/2) + erf(n-iC/2)) \tag{72}$$

$$\int_0^n d\eta e^{-\eta^2}\sin(C\eta) = \frac{\sqrt{\pi}e^{-C^2/4}}{4i}\left(erf(n-iC/2) - erf(n+iC/2) + 2erf(iC/2)\right) \tag{73}$$

Proof. **1)** Using Euler's formula we get

$$\begin{aligned}\int_0^n d\eta e^{-\eta^2}\cos(C\eta) &= \int_0^n d\eta e^{-\eta^2}\frac{e^{iC\eta}+e^{-iC\eta}}{2}\\ &= \int_0^n d\eta\frac{e^{-\eta^2+iC\eta}+e^{-\eta^2-iC\eta}}{2}\end{aligned}$$

Notice that by completing the square:

$$(\eta \pm iC/2)^2 = \eta^2 \pm iC\eta - C^2/4$$

Preparing substitution;

$$\begin{aligned}-\eta^2 + iC\eta &= -(\eta - iC/2)^2 - C^2/4 = -\eta_1^2 - C^2/4\\ \eta \in [0,n] &\iff \eta_1 \in [0 - iC/2, n - iC/2]\\ -\eta^2 - iC\eta &= -(\eta + iC/2)^2 - C^2/4 = -\eta_2^2 - C^2/4\\ \eta \in [0,n] &\iff \eta_2 \in [0 + iC/2, n + iC/2]\end{aligned}$$

Substitution gives:

$$\begin{aligned}\int_0^n d\eta e^{-\eta^2+iC\eta} &= \int_{0-iC/2}^{n-iC/2} d\eta_1 e^{-\eta_1^2 - C^2/4}\\ &= e^{-C^2/4}\int_{0-iC/2}^{n-iC/2} d\eta_1 e^{-\eta_1^2}\\ &= \frac{\sqrt{\pi}e^{-C^2/4}}{2}(\operatorname{erf}(n-iC/2) - \operatorname{erf}(-iC/2))\end{aligned}$$

Now the other term, which of course goes similar:

$$\begin{aligned}\int_0^n d\eta e^{-\eta^2 - iC\eta} &= \int_{0+iC/2}^{n+iC/2} d\eta_2 e^{-\eta_2^2 - C^2/4} \\ &= e^{-C^2/4} \int_{0+iC/2}^{n+iC/2} d\eta_2 e^{-\eta_2^2} \\ &= \frac{\sqrt{\pi} e^{-C^2/4}}{2} (\mathrm{erf}(n + iC/2) - \mathrm{erf}(iC/2))\end{aligned}$$

Putting it all together:

$$\begin{aligned}2\int_0^n d\eta e^{-\eta^2} \cos(C\eta) &= \frac{\sqrt{\pi} e^{-C^2/4}}{2} (\mathrm{erf}(n - iC/2) - \mathrm{erf}(-iC/2)) \\ &+ \frac{\sqrt{\pi} e^{-C^2/4}}{2} (\mathrm{erf}(n + iC/2) - \mathrm{erf}(iC/2)) \\ &= \frac{\sqrt{\pi} e^{-C^2/4}}{2} (\mathrm{erf}(n + iC/2) + \mathrm{erf}(n - iC/2))\end{aligned}$$

2) Now for the sine-integral. Using Euler's formula we get:

$$\int_0^n d\eta e^{-\eta^2} \sin(C\eta) = \int_0^n d\eta \frac{e^{-\eta^2 + iC\eta} - e^{-\eta^2 - iC\eta}}{2i}$$

The substitution steps we don't have to repeat again, there's only some different constant involved.

$$\begin{aligned}2i\int_0^n d\eta e^{-\eta^2} \sin(C\eta) &= \frac{\sqrt{\pi} e^{-C^2/4}}{2} (\mathrm{erf}(n - iC/2) - \mathrm{erf}(-iC/2)) \\ &- \frac{\sqrt{\pi} e^{-C^2/4}}{2} (\mathrm{erf}(n + iC/2) - \mathrm{erf}(iC/2)) \\ &= \frac{\sqrt{\pi} e^{-C^2/4}}{2} (\mathrm{erf}(n - iC/2) - \mathrm{erf}(n + iC/2) + 2\mathrm{erf}(iC/2))\end{aligned}$$

□

Definition C.2. Let's define for $C, \varphi \in \mathbb{R}$

$$O_C^\varphi(n) := \int_0^n d\eta e^{-\eta^2} \sin(C\eta + \varphi) \tag{74}$$

$$E_C^\varphi(n) := \int_0^n d\eta e^{-\eta^2} \cos(C\eta + \varphi) \tag{75}$$

Corollary C.1 (Interpolation)**.**

$$\begin{aligned}O_C^\varphi(n) = \cos(\varphi) \frac{\sqrt{\pi} e^{-C^2/4}}{4i} (erf(n - iC/2) - erf(n + iC/2) + 2erf(iC/2)) \\ + \sin(\varphi) \frac{\sqrt{\pi} e^{-C^2/4}}{4} (erf(n - iC/2) + erf(n - iC/2))\end{aligned}$$

And

$$E_C^\varphi(n) = O_C^{\varphi + \pi/2}(n)$$

Proof. This follows from $\sin(C\eta + \varphi) = \cos(\varphi)\sin(C\eta) + \sin(\varphi)\cos(C\eta)$. □